

# Hybrid bilayer membranes as platforms for biomimicry and catalysis

Tian Zeng o¹, Rajendra P. Gautam², Danny H. Ko o³, Heng-Liang Wu⁴,⁵, Ali Hosseini³, Ying Li¹, Christopher J. Barile², and Edmund C. M. Tse o¹.

Abstract | Hybrid bilayer membrane (HBM) platforms represent an emerging nanoscale bio-inspired interface that has broad implications in energy catalysis and smart molecular devices. An HBM contains multiple modular components that include an underlying inorganic surface with a biological layer appended on top. The inorganic interface serves as a support with robust mechanical properties that can also be decorated with functional moieties, sensing units and catalytic active sites. The biological layer contains lipids and membrane-bound entities that facilitate or alter the activity and selectivity of the embedded functional motifs. With their structural complexity and functional flexibility, HBMs have been demonstrated to enhance catalytic turnover frequency and regulate product selectivity of the O<sub>2</sub> and CO<sub>2</sub> reduction reactions, which have applications in fuel cells and electrolysers. HBMs can also steer the mechanistic pathways of proton-coupled electron transfer (PCET) reactions of quinones and metal complexes by tuning electron and proton delivery rates. Beyond energy catalysis, HBMs have been equipped with enzyme mimics and membrane-bound redox agents to recapitulate natural energy transport chains. With channels and carriers incorporated, HBM sensors can quantify transmembrane events. This Review serves to summarize the major accomplishments achieved using HBMs in the past decade.

There is a growing demand for biocompatible metal surfaces in various research fields such as in electrochemistry<sup>1-3</sup>, biosensors<sup>4-6</sup>, catalysis<sup>7-9</sup> and wearable technology<sup>10-12</sup> (FIG. 1a). A hybrid bilayer membrane (HBM) is an inorganic-organic electrochemical platform in which a lipid layer is appended on top of a self-assembled monolayer (SAM) covalently attached to a substrate<sup>13,14</sup>, which has diverse functions and broad applications in the fields of biomimicry and catalysis. The basic HBM system consists of three parts — the lipid layer, the SAM and the substrate<sup>15,16</sup> (FIG. 1b). 'Hybrid' refers to the combination of artificial (inorganic substrates and metal ions) and natural (lipids and receptors) components. 'Bilayer' indicates that two dissimilar layers are covering the surface. In HBMs, the lipid (membrane) layer is typically a phospholipid and is affixed to the surface via van der Waals interactions between the lipid tails and the terminal functionalities of the SAMs<sup>17,18</sup>. The modularity of each HBM component allows them to be tuneable. For example, the HBM platform can be used to immobilize biological materials on surfaces and is typically stable for at least a few weeks<sup>19</sup>. By constructing HBMs on conductive metal surfaces, HBM platforms can be explored using techniques that have not previously been possible with traditional biological

membranes<sup>20,21</sup>. Also, not being bound by biological systems allows the membrane attributes of HBMs to be controlled more easily than a pure biological membrane. The ability to tune membrane components endows HBMs with the biocompatibility needed for functional transmembrane studies. The opportunity to regulate the proton and electron transfer steps independently has led to unprecedented insights into the molecular details that govern activity and selectivity of multistep redox catalysts central to renewable energy schemes<sup>13,18,22,23</sup>.

#### **Types of HBM**

There are various kinds of model membrane that have been used in biomimetic research (BOX 1). These membranes can be produced in different forms, such as lipid vesicles<sup>24</sup>, bilayer lipid membranes<sup>25</sup>, Langmuir–Blodgett layers<sup>26</sup>, black lipid membranes<sup>27</sup>, and tethered and nontethered supported planar bilayers<sup>28</sup>. The main components of model membranes are amphiphilic phospholipids, which consist of hydrophobic alkane chains and polar phosphate head groups.

In HBMs, the SAM can be a simple redox inactive system like alkanethiols on Au (REFS. <sup>13,16</sup>), or they can attach a redox-active molecule like ferrocene on alkanethiols <sup>21</sup>, or they can contain a larger catalyst unit such as a

<sup>1</sup>Department of Chemistry, University of Hong Kong, Hong Kong SAR, China.

<sup>2</sup>Department of Chemistry, University of Nevada, Reno, NV, USA.

<sup>3</sup>Catalyst Tec Limited, Auckland, New Zealand.

<sup>4</sup>Center for Condensed Matter Sciences, National Taiwan University, Taipei, Taiwan.

<sup>5</sup>Center of Atomic Initiative for New Materials, National Taiwan University, Taipei,

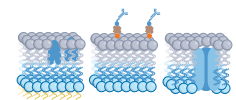
<sup>™</sup>e-mail: ali.hosseini@ catalysttec.com; yingli0e@ hku.hk; cbarile@unr.edu; ecmtse@hku.hk

https://doi.org/10.1038/ s41570-022-00433-2

a Artificial and natural



- Designer platformsSurfaces and nanoparticles
- Fluidity, stability, sensitivity



Catalysis, energy sensingAdvanced applications

Molecular self-assembly



Interfacial functionalization
Biomimicry

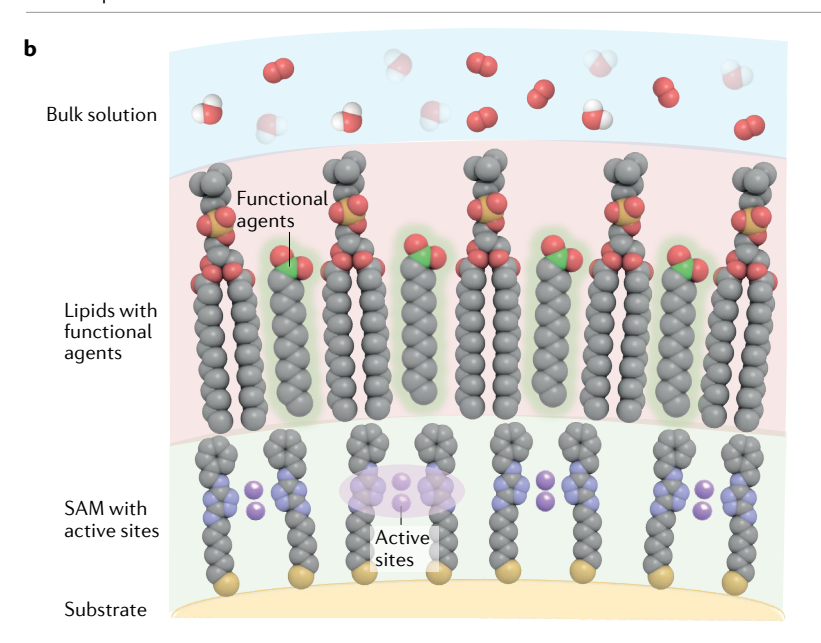


Fig. 1 | **HBM platforms at a glance. a** | An overview of hybrid bilayer membrane (HBM) topics discussed throughout this Review. **b** | Overall structure of HBM, highlighting its functional components. SAM, self-assembled monolayer. Part **b** adapted with permission from REF. $^{36}$ , ACS.

coordination compound or an enzyme mimic $^{29-31}$ . The lipid layers in HBMs can be lipid monolayers or bilayers, both of which can be constructed using self-assembly techniques<sup>16,32</sup>. In HBMs with lipid monolayers, hydrophobic SAMs (usually methyl- or aryl-terminated) associate with the hydrophobic tails of the lipid layer. In contrast, in HBMs with lipid bilayers, hydrophilic SAMs (carboxylate-terminated) associate with the hydrophilic phosphate head groups on one leaflet of the lipid bilayer. Compared to the HBMs with lipid monolayers, bilayer structures are more dynamic and fluxional33,34. Thus, HBMs with lipid bilayers can provide a better model system for biological processes. However, if stability is crucial, HBMs with lipid monolayers are preferred, which is why these have been investigated much more for energy catalysis applications than those with lipid bilayers. Furthermore, for many aspects of biomimicry, the lipid monolayer-SAM interface serves as a sufficient model of biological lipid bilayers<sup>22,35,36</sup>. Nonetheless, it is important for researchers to be aware of possible spontaneous lipid bilayer formation while working with HBMs. The differentiation between monolayer and bilayer structures can easily be determined with ellipsometry, which can be used to calculate the distance between the inorganic electrode and the electrolyte-HBM interface. In short, functional mimics for bio-inspired catalysis probably use monolayers, while bilayers serve as valid structural mimics of authentic biological systems.

The most frequently used substrate to construct HBMs is Au (REFS. 13,16), but other substrates (such as carbon<sup>37</sup>, Ag (REF.<sup>25</sup>), Si (REF.<sup>24</sup>), Hg (REFS.<sup>33,38</sup>) and Al (REF. 39)) have also been exploited. In principle, any conductive substrate can be used for electrochemical applications<sup>40-44</sup>. Au is often preferred because of its inertness, its well defined surface morphology, its ability to form robust Au-S bonds for thiol-based SAMs, and its reflectivity, which makes it useful for surface-characterization techniques such as ellipsometry and polarization modulation-infrared reflectionabsorption spectroscopy (PM-IRRAS)45,46. On Au, alkanethiols usually form tightly packed and well ordered monolayers with a fairly wide electrochemical window. This potential window can vary depending upon the thiol of choice, but typically ranges from +0.8 V to -0.5 V versus Ag/AgCl.

#### The utility of HBM platforms

HBMs were initially developed as bioinspired platforms on an electrode support to study cell membrane activity and associated processes<sup>47,48</sup>. Over the past three decades, HBM and tethered bilayer lipid membranes on solid supports have attracted much attention as a means of studying a broad range of fundamental and applied fields49. This increase in popularity is due to their ability to mimic cell membranes, which is similar to that of Langmuir-Blodgett films and black bilayer lipid membranes, but they have a number of added advantages including simpler and reproducible preparation, increased stability and improved precision in controlling their composition and architecture<sup>50</sup>. Their formation on a solid and/or conductive support also allows a wider range of analytical techniques to be employed that were not previously accessible<sup>51-53</sup>. The continual evolution of HBMs has expanded their applications to include the investigation of molecular recognition in cell membranes<sup>54,55</sup>, ion permeability<sup>56</sup>, enzymatic activity<sup>57,58</sup>, cell adhesion<sup>50,59</sup>, electrocatalysis<sup>18,22</sup>, photoelectric effects<sup>60,61</sup>, functionalization of beads<sup>62</sup>, biosensors<sup>63,64</sup> and reversed-phase chromatography for separation<sup>65</sup>.

Predominantly, HBMs have been developed as platforms that can mimic native membranes in order to gain unique insights into membrane functions and proteins<sup>13</sup>. Many of these proteins are either redox enzymes that are involved in biological energy conversion processes, such as metabolism, which operates in the mitochondrial membranes, photosynthesis, which operates in the chloroplast membranes, or they are channels and voltage-gated transporters, regulating cellular functions<sup>29</sup>. These redox proteins can also mediate electron transport and catalyse other important reactions in both biological and industrial applications<sup>66,67</sup>. Most importantly, dysfunction in enzymatic activity and aberrant channels can lead to physiological disorders<sup>68,69</sup>. As a result, it is essential to develop a fundamental understanding of their biological functions, and HBMs can aid in relevant mechanistic studies<sup>59,70</sup>.

At a molecular level, the active site of redox proteins is embedded in the hydrophobic matrix created by the protein, where the transport of charged species, such as electrons and protons, is tightly regulated 71,72.

The convergent preparation of HBMs allows for independent control over the composition and dispersion of species of interest within each leaflet. This feature has made it possible to evaluate redox processes with atomic precision in a hydrophobic environment and to construct analogues of proteins that were not previously accessible.

HBMs embedded with a molecular catalyst have enabled the in-depth analysis of proton-coupled electron transfer (PCET) reactions, which are central to many biological and artificial energy conversion processes <sup>13,73</sup>. In particular, HBMs allow for precise control over the thermodynamics and kinetics of proton and electron transfer steps in PCET processes <sup>22,23</sup>. These electrochemical platforms have led to a deeper understanding of the parameters influencing the efficiency of catalytic processes <sup>36,74</sup>.

Recently, HBMs have proved to be a powerful tool with which to examine photoelectrochemical properties in an environment that closely mimics natural photosystems<sup>75</sup>. Inspired by the antenna system of chlorophyll situated in biological membranes, dye molecules tailored for visible light absorption can be installed at the phospholipid-alkanethiol interface of HBMs to construct new dye-sensitized solar cells for natural solar absorption and efficient charge separation<sup>60,61</sup>. Compared to earlier lipid models, HBM nano-assembly displays the robustness required owing to the stability provided by the electrode support. The independently controllable HBM leaflets allow designer electron donor/acceptor pairs including fullerenes, [Ru(bpy)<sub>3</sub>]<sup>2+</sup> and porphyrins to be incorporated modularly at specific locations in HBMs. This modularity results in directed vectorial charge transfer across the two dissimilar layers in HBMs and efficient light energy harvesting<sup>76</sup>. In addition to enabling the study and evaluation of many combinations of donor-acceptor systems, this unique design of HBMs achieves high photoconversion efficiency. The lipid

Box 1 | Model membranes used in biomimetic research

H'
H'
Vesicle
H'
Lipid vesicles

Langmuir–Blodgett layers

Black lipid membranes

S S S S

Bilayer lipid membranes

Tethered and nontethered supported planar bilayers

matrix acts as an effective barrier, suppressing undesired charge recombination, leading to efficient initial photo-induced electron transfer and subsequently notable enhancement in photoconversion<sup>75</sup>. The photocurrents generated by HBMs can be further modulated through quantitative addition of molecular photosensitizing agents into the lipid matrix to regulate light-induced cross-membrane electron-transfer processes<sup>60</sup>. This distinctive construction of photosystem-mimicking HBM systems has provided insights into and understanding of photo-induced charge transfer and separation, which are crucial to the development of more advanced photovoltaic devices<sup>77</sup>.

Beyond a fundamental understanding of biological and molecular processes, HBMs have also been considered for a number of commercial applications. These platforms have increased the diversity of transduction methods (optical, electrochemical, and quartz crystal or surface acoustic wave oscillators) available as a result of their intrinsic properties 76,78,79. This feature, combined with their biocompatibility and their ability to anchor biological capture agents without chemical transformation or covalent modification, has opened up the development of a novel class of bioanalytics that could lead to higher sensitivity, enhanced specificity and lower cost 80-83.

The self-assembled hydrophobic environments in HBMs have led to optimization of reverse-phase columns for more efficient separation of species of interest<sup>65</sup>. HBMs have also been considered as a tool with which to tune the dielectric properties of Au-coated polymer microspheres, which can be used as labels, carriers and solid supports for the separation and analysis of chemical, biochemical and biological analytes<sup>84,85</sup>.

Biomimicry and energy catalysis have co-evolved in the past years, and the shared properties of HBMs have led to discoveries and improvements in both fields in a synergistic fashion (FIG. 2). Through biomimicry, bioinspired catalysts with improved performance have been developed. These successes in turn facilitate the design of new structural and functional mimics of biological systems, thereby forming a feedback loop and closing the design-build-test-learn cycle of HBM platforms.

This Review first covers the preparation methods of inorganic-organic HBMs and the techniques used to characterize such HBMs. The remaining portion of this Review describes the practical applications of these abiotic-biotic HBMs as well as future challenges in the field of HBMs. Readers may refer to other reviews for detailed discussions of lipid vesicles and their uses in artificial cells, therapeutics and drug delivery<sup>86–89</sup>.

#### **Preparation and characterization**

The chemical synthesis and material characterization of HBM modular components are described in this section (FIG. 3a).

Self-assembled monolayers. Initial studies focused on using the Au–S system to form the SAM in an HBM<sup>21,90,91</sup>. The SAM molecule features three functional units that include a terminal thiol functional group for SAM formation, a moiety in the middle for catalyst integration, and a benzyl group on the other end for

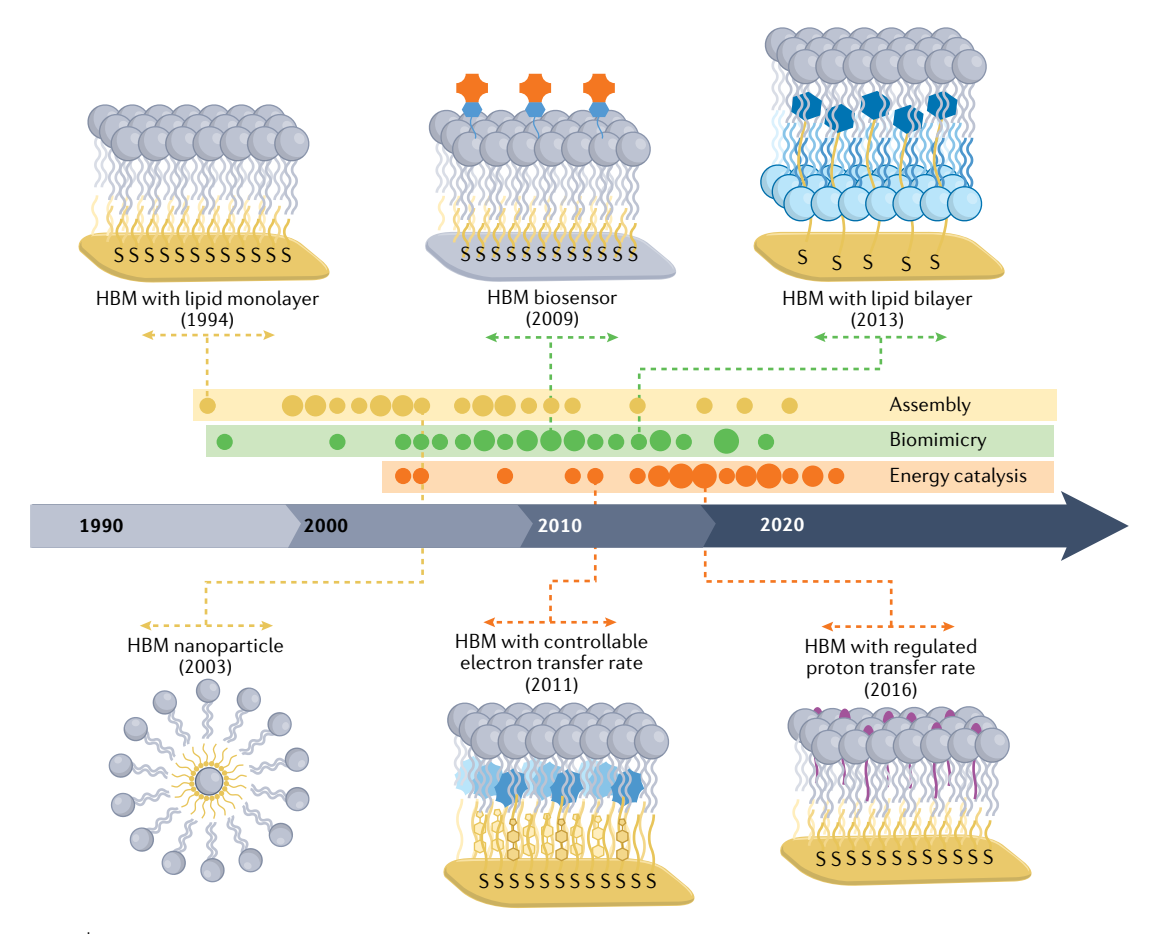


Fig. 2 | **HBM development timeline.** Timeline of the development of the hybrid bilayer membrane (HBM) field organized by advances in assembly, biomimicry and energy catalysis.

lipid appendage<sup>92,93</sup>. First, trityl protecting groups, which can be removed under acidic conditions, are introduced to prevent the free thiol from reacting throughout the synthesis<sup>18</sup>. Typically, a pre-rinsed electrode is soaked in a methanolic or ethanolic solution containing the deprotected molecule to generate a SAM<sup>22</sup>. Depending on the molecular architecture of the target system, this soaking process can be performed in the dark under an inert atmosphere for greater control over the SAM-formation environment<sup>94</sup>. A linker, comprised of between 4 and 8 methylene units, is used to connect the thiol to the catalyst motif, which should allow for efficient charge migration between the Au electrode and the catalyst moiety<sup>56</sup>. In general, a longer linker results in higher robustness but with a decreased electron transfer rate<sup>23</sup>.

Second, the supporting ligand of the catalyst moiety can be incorporated via covalent attachment prior to SAM formation or through late-stage functionalization using click chemistry<sup>23</sup>. For both methods, metal ions are subsequently coordinated to the ligand-containing SAM by soaking the SAM in a methanolic or ethanolic solution containing the desired transition metal<sup>95</sup>. For example, a redox non-innocent triazole ligand has been covalently attached to a SAM that included an active dicopper oxygen reduction reaction (ORR) electrocatalyst<sup>18</sup>. Third, a benzyl group is conjugated to the terminal amine group of this SAM system to achieve a surface with suitable hydrophobicity to allow for lipid layer formation in

order to generate an HBM (FIG. 3b). In short, trifunctional SAMs with precise molecular structures are designed to enable efficient assembly of the bottom layer of HBMs.

Tethered redox moieties. In addition to the Cu triazole system, a variety of other redox-active scaffolds have been installed at the SAM terminus. These scaffolds include Fe porphyrins<sup>13</sup>, quinones<sup>73</sup>, and ferrocenes<sup>21</sup>, which do not rely on two adjacent triazole ligands to chelate two Cu ions in a cooperative fashion. These redox moieties were attached to alkanethiols using C-C bond cross-coupling, copper-catalysed azide-alkyne cycloaddition or amide bond-forming strategies (using common coupling agents), in which corresponding molecular handles were previously installed at the SAM terminus (FIG. 3c,d). Beyond building systems with varying catalytic attributes and accessing tethered units with varying redox potentials, these site-isolated redox SAMs allow for HBMs to be constructed on rough or curved interfaces displaying various surface functionalities%. Therefore, HBMs can be fabricated on non-Au substrates as well as on nanoparticles34,97. The solvent and dispersant used during synthesis need to be chosen to avoid agglomeration when preparing nanoparticle-based HBMs<sup>98</sup>. Clickable lipids with attachable motifs can be covalently attached to SAMs to enhance the robustness of HBM constructs<sup>99,100</sup>. In summary, these design strategies can afford modular and stable HBMs.

### Agglomeration A process in which

A process in which nanoparticles aggregate into a larger mass that is loosely packed by physical and chemical forces. Bioinspired proton carriers. Proton carriers are key components of HBM systems that achieve regulation of proton delivery under desirable conditions (FIG. 3e,f). With careful molecular design, proton carriers can operate within designated pH ranges<sup>22</sup>, be activated with light94 and function with different transmembrane mechanisms<sup>36</sup>. Inspired by biological systems, carboxylic acids with long carbon tails were initially chosen for HBM investigations<sup>13</sup>. The appropriate carbon chain length allows this type of proton carrier to fulfil proton delivery<sup>15</sup>. In HBMs with triazole scaffolds, boronic acids showed dose-dependent proton delivery capability<sup>22</sup>. This boronic acid motif has been incorporated into a photo-responsive proton carrier using a stiff stilbene moiety94, which turns on upon irradiation with 360-nm light and shuts down upon treatment with 390-nm light. Recently, cyanide groups have been used as proton carriers, which parallels their utility as protonophores in mitochondria<sup>36</sup>. The proton-shuttling ability of alkyl cyanides has been studied in HBM systems. To explore the transmembrane proton delivery mechanism, derivatives of alkyl cyanides were synthesized through substituting the alpha protons with methyl groups and deuterons.

**Vesicle fusion method.** Vesicle fusion is usually used to append a lipid layer on top of a SAM-modified electrode to generate an HBM platform  $^{101}$ . Lipid and proton carriers are dissolved in chloroform or ethanol and then dried under a stream of  $N_2$  or Ar to generate a uniform film  $^{13,21}$ . Isopropyl alcohol or ethanol is then added to re-dissolve the film, followed by buffer addition and sonication  $^{18,22}$ . The SAM-modified electrode is then soaked in the as-prepared lipid-forming solution to generate an HBM via vesicle fusion  $^{36,95}$ . Enzymes and proteins can be incorporated into an HBM in all stages of its preparation  $^{25,102,103}$ . They can be tethered directly onto the electrode surface

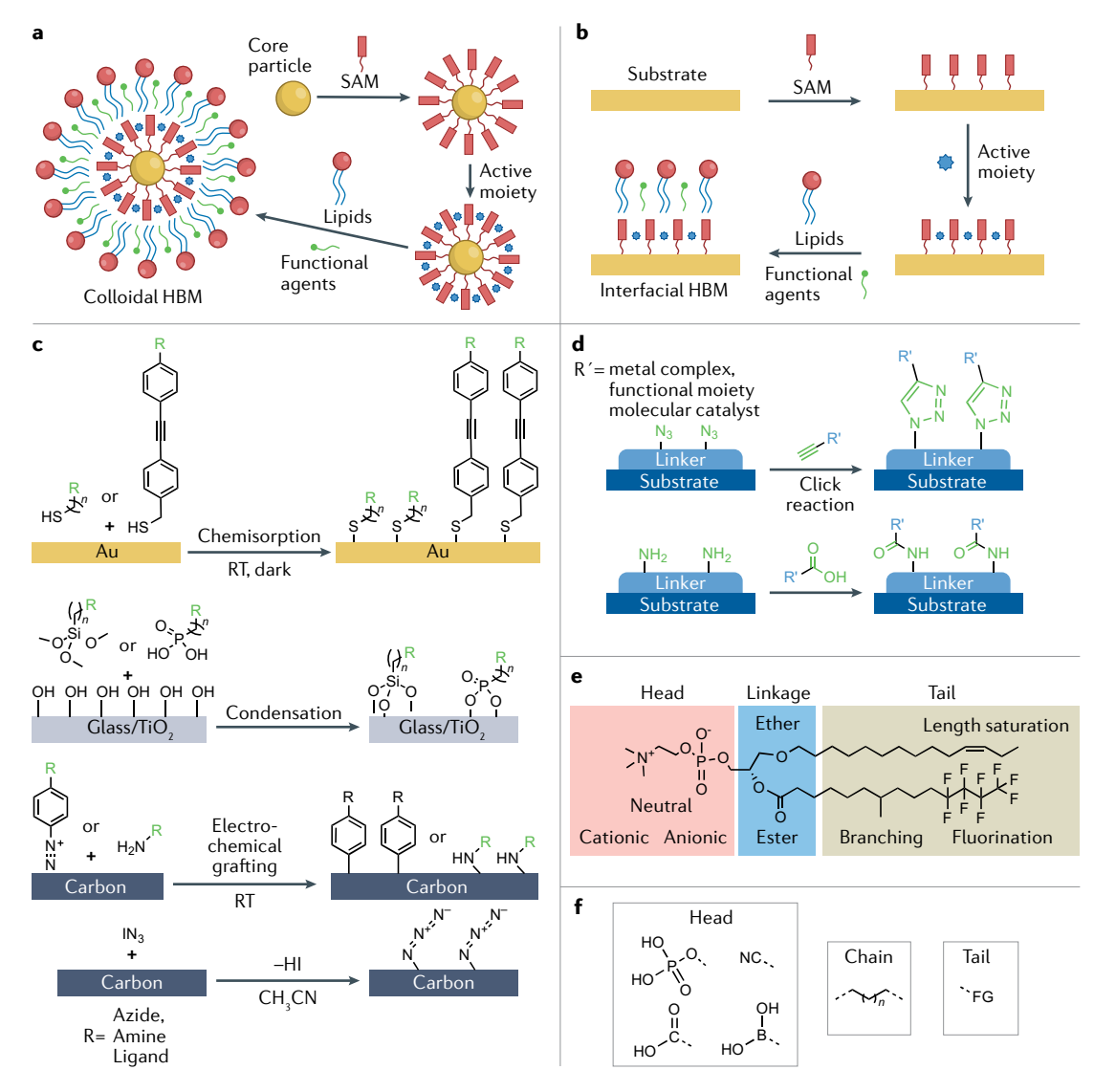


Fig. 3 | **HBM preparation schemes.** a | Colloidal hybrid bilayer membrane (HBM) preparation workflow. b | Interfacial HBM preparation workflow. c | Chemical strategies for surface modification of the solid support. d | Self-assembled monolayer (SAM) functionalization using click chemistry and amide coupling. e | Components selected on lipids for tuning membrane properties. f | Functional molecules that can be embedded in membranes for biomimicry and energy catalysis. RT, room temperature.

#### Box 2 | HBM characterization techniques

X-ray photoelectron spectroscopy (XPS) is a technique for measuring the elemental composition and oxidation state of the elements on hybrid bilayer membrane (HBM) surfaces.

Electrochemical impedance spectroscopy (EIS) is a technique for measuring the resistance and capacitance of HBM films with the help of equivalent circuit models. Subsequently, the thickness of HBMs can then be deduced.

Atomic force microscopy (AFM) is a non-optical nanoscale imaging scanning probe technique that characterizes the surface morphology and mechanical properties of HBMs. The thickness of HBMs can be quantified using AFM-based force curve measurement.

Sum frequency generation (SFG) spectroscopy takes advantage of a second-order nonlinear optical process to analyse the chemical structure of asymmetric HBM interfaces.

Polarization modulation-infrared reflection-adsorption spectroscopy (PM-IRRAS) is a vibrational spectroscopic technique that probes the stretching and bending modes of HBMs on reflective metal substrates with high surface sensitivity.

Surface-enhanced Raman spectroscopy (SERS) is a Raman scattering technique that probes the vibrational modes of HBMs supported on plasmonic nanomaterials.

Surface plasmon resonance (SPR) is a label-free technique used to monitor noncovalent molecular interactions in a non-invasive fashion to quantify the binding affinities and association-dissociation kinetics of target substrates onto bioreceptors present at the liquid-lipid interface of HBMs in real time.

Ellipsometry is an optical technique that determines the polarization state change, the dielectric property and the thickness of HBM thin films.

prior to HBM formation. They can also be incorporated by vesicle fusion, where the vesicles can be populated with proteins either by reconstitution or during its formation. Alternatively, the proteins can be reconstituted into the HBM platform. The reconstitution of vesicles prior to their fusion onto the hydrophobic self-assembled surface typically enables better control for the immobilization of the contents of a cell membrane, such that proteins, enzymes, lipids and receptors are oriented correctly.

Surface probing methods. HBMs have been characterized using a suite (BOX 2) of chemical and physical methods (FIG. 4). To probe their surface composition, X-ray photoelectron spectroscopy (XPS) has been used to reveal the identity and oxidation state of the elements present on HBM platforms<sup>95</sup>. To measure the HBM thickness, ellipsometry is the method of choice<sup>18</sup>. Electrochemical impedance spectroscopy (EIS) can also deduce the HBM thickness by modelling the film capacity and resistance<sup>25,52,106</sup>. Atomic force microscopy (AFM) can image the surface morphology of HBMs as well as further investigate the mechanical properties of HBMs via force curve measurements<sup>106</sup>. To analyse the chemical structure of HBMs, sum frequency generation (SFG) spectroscopy<sup>107,108</sup>, PM-IRRAS<sup>45,46</sup>, transmission IR spectroscopy<sup>109</sup>, and surface-enhanced Raman spectroscopy (SERS)<sup>110</sup> have been utilized to monitor the vibrational and bending modes of resting-state species, bound adducts, and catalytic intermediates present on HBMdecorated surfaces. To study the interaction of solution species with receptors on HBMs, surface plasmon resonance (SPR) and electrochemistry have been used to quantify the binding affinities and association kinetics<sup>111</sup>.

HBM architecture progress. Earlier work discussed the use of alkanethiol SAM on Au surfaces as a starting point for the formation of stable, biomimetic HBMs<sup>16</sup>.

Later, ferrocene-embedded HBMs were used to study the redox properties and membrane permeability of solution-phase redox-active molecules 112,113. Neutron reflectometry has been used to measure the dimensions and analyse the structures of HBMs containing the peptide melittin<sup>14</sup>. Beyond using precious-metal substrates for HBMs, HBMs have been constructed on carbon surfaces, and offer wider electrochemical windows than those formed on Au (REF. 37). Such carbon-based HBMs were used to study the transport of alkali ions through lipid layers modified with valinomycin, a peptide that functions as a potassium ion channel in cells. Additionally, a procedure for forming HBMs on Al surfaces has also been developed<sup>39</sup>. In this HBM system, the phospholipid layers are deposited on self-assembled silane monolayers. Through constructing HBMs consisting of octadecanethiol SAMs on surface-roughened Ag electrodes. HBMs have been used in surface spectroscopy to analyse interfacial processes<sup>110</sup>. The next section discusses how these various HBM architectures can be used for biomimicry and catalysis, and highlights the prospects of these approaches.

#### Applications of HBMs

Catalysis for renewable energy. Renewable energy devices have attracted much attention because they provide a feasible route to transition the global energy economy to clean and sustainable resources  $^{114-122}$ . Many of these devices rely on the electrocatalysis of small molecules such as  $\rm O_2$  and  $\rm CO_2$  (REFS.  $^{123-128}$ ). For example, the ORR to water occurs at the cathode of fuel cells  $^{129-135}$ , and the reduction of  $\rm CO_2$  to fuels such as methane and methanol could be instrumental in designing future devices that convert carbon emissions to value-added products  $^{136-141}$ .

The electrocatalysis of these small molecules involves the transfer of multiple protons and electrons <sup>142–145</sup>, the dynamics of which affect catalyst selectivity <sup>146–148</sup>, efficiency <sup>149–151</sup>, turnover frequency <sup>152,153</sup>, and durability <sup>154,155</sup>. Electron- and proton-transfer events can occur in a stepwise fashion, or simultaneously in what is known as PCET <sup>156–164</sup>. The complex mechanistic possibilities of these reactions have made them difficult to study and has stymied the progress of catalyst development for renewable energy applications. Therefore, it is important to explore new routes that may afford additional insights into the design and reactivity of PCET catalysts. Indeed, the HBM platform may well aid in catalyst design.

HBMs on electrodes offer a unique method of studying the electrocatalysis of small molecules relevant to renewable energy devices. In particular, HBM platforms can be used to modulate the thermodynamics and kinetics of electron and proton transfer to an appended catalyst<sup>18,22</sup>. In any electrochemical system, the thermodynamics of electron transfer can easily be modulated by changing the voltage applied via a potentiostat. For most metal-centred catalysts, the thermodynamics of proton transfer can also be changed by altering the pH of the bulk solution<sup>165,166</sup>. Through the Nernst equation, the redox potential of the metal centre and correspondingly of catalysis is shifted through pH changes<sup>95</sup>. Moreover,

#### Flip-flop diffusion

A process where a bilayerbound molecule moves from one lipid leaflet to another leaflet the kinetics of electron transfer can be modulated using SAMs of different alkyl chain lengths in an HBM<sup>21,23</sup>. SAMs with longer alkyl chain lengths possess slower electron transfer rates because electrons from the electrode must tunnel through the insulating methylene groups of the SAM to reach the catalyst<sup>167,168</sup>. Last, proton-transfer kinetics can be tuned by changing he proton permeability of the lipid layer in the HBM<sup>15,18,22</sup>. In biological lipid bilayers, it is known that proton carriers such as alkyl carboxylates transfer protons across membranes via flip-flop diffusion<sup>52,169,170</sup>. HBMs can provide a

unique framework in which to simultaneously control four key parameters of PCET reaction dynamics — the thermodynamics and kinetics of both proton and electron transfer — in one streamlined electrode architecture. In the context of renewable energy catalysis, the ability to tune these reaction attributes has enabled HBMs to elucidate PCET reaction mechanisms and increase product selectivity in ways that are not possible with conventional electrodes.

As a first demonstration, a SAM of site-isolated Fe porphyrin was pre-organized on a Au electrode<sup>13</sup> (FIG. 5a).

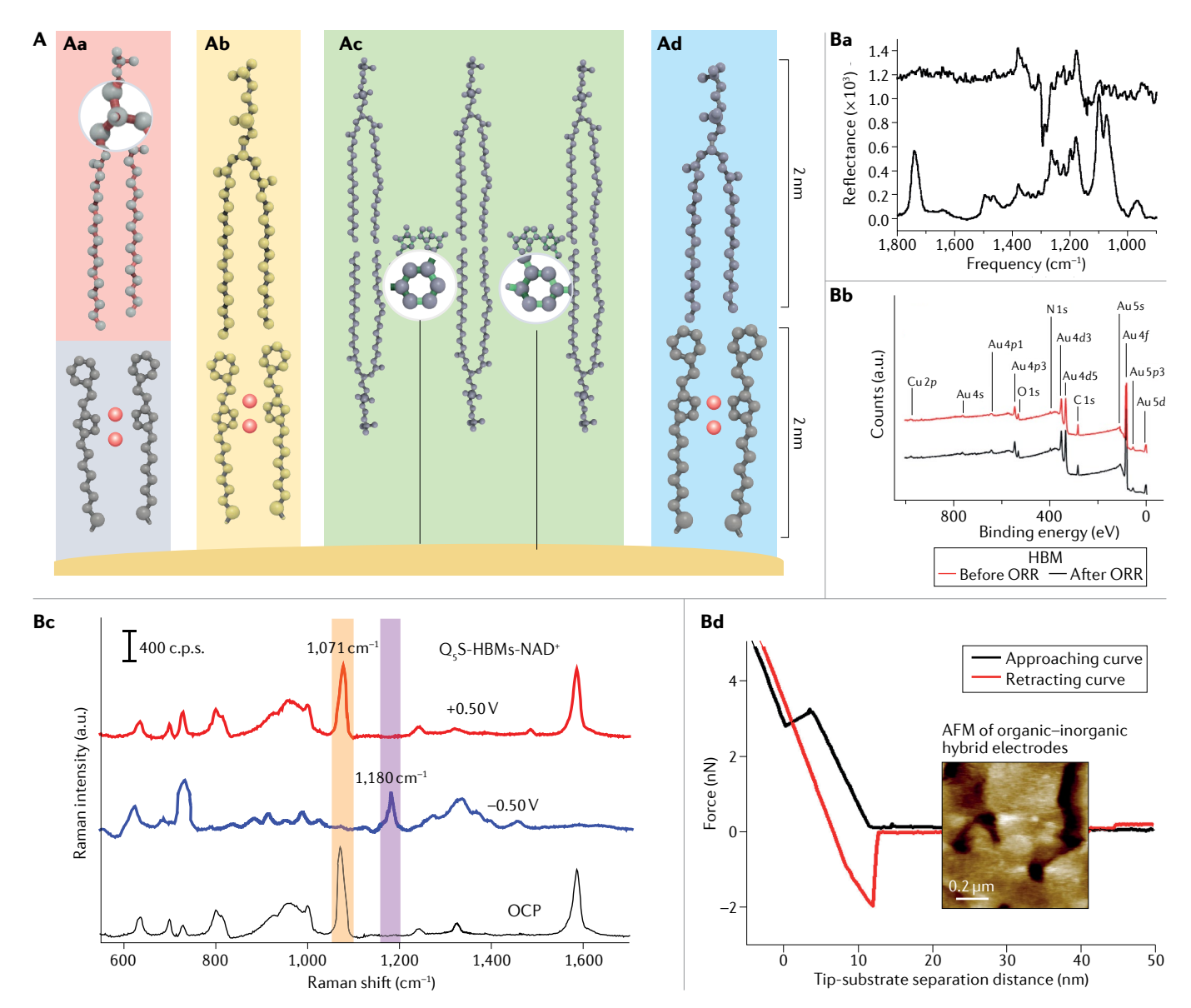
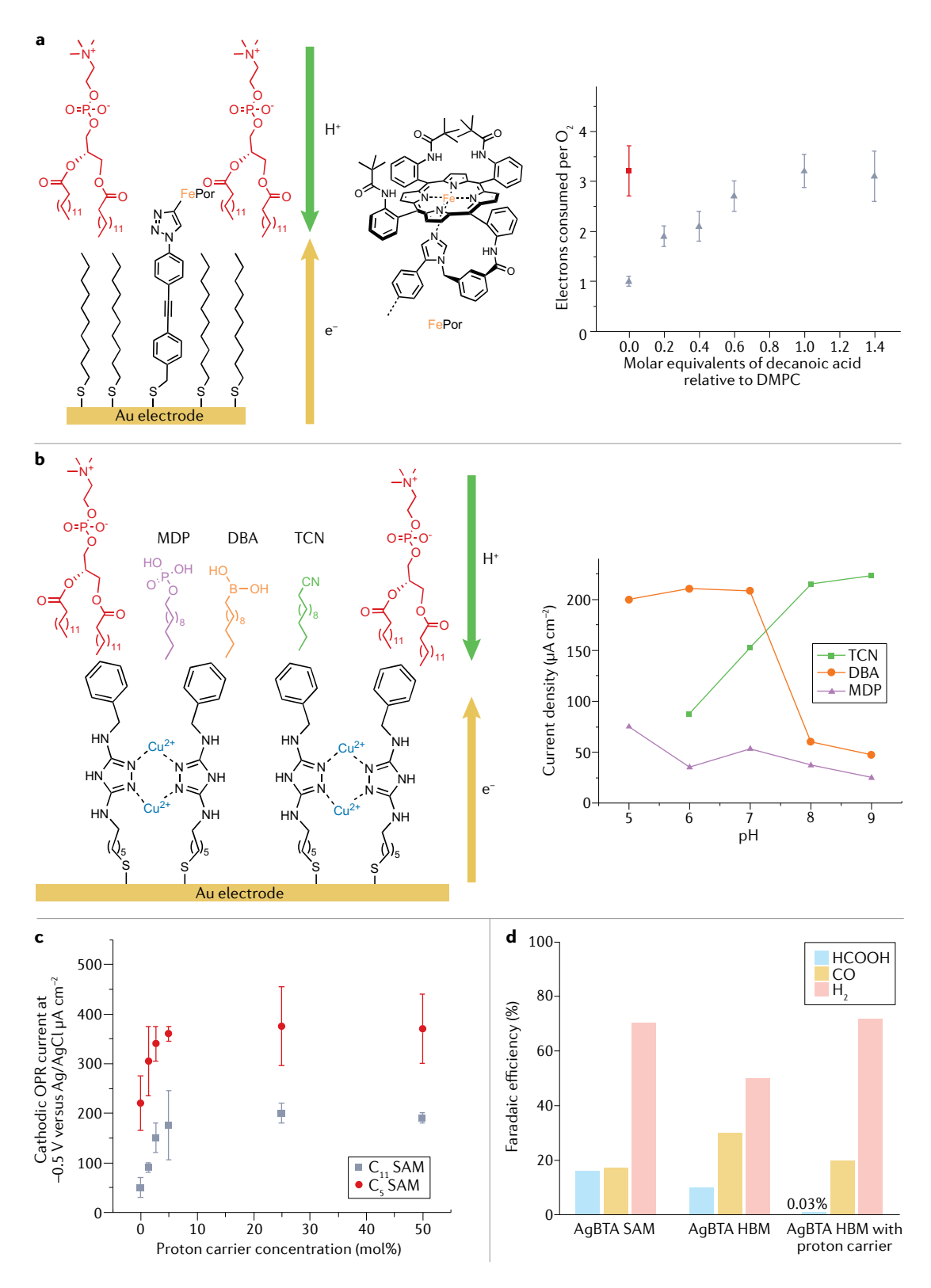


Fig. 4 | Morphological and compositional characterization of HBMs. A | Schematic showing the characteristics of hybrid bilayer membranes (HBMs) that can be measured. Aa | Vibrational modes. Ab | Stretching and bending modes. Ac | Atomic composition. Ad | Thickness. Stretching and bending can be determined using infrared and Raman spectroscopies. Chemical identity and oxidation states of select elements in HBMs can be determined using X-ray photoelectron spectroscopy. The thickness of the different layers can be determined using atomic force microscopy. B | Spectroscopic measurements and morphological probing of HBM surfaces. Ba | Changes in the SERS bands as a function of the applied potential

on an HBM electrode. **Bb** | PM-IRRAS spectrum of an HBM (top). Difference spectrum of bands associated with the phospholipid acyl chains by subtracting the deuterated signal from the hydrogenated signal (bottom). **Bc** | X-ray photoelectron spectroscopy (XPS) survey scan of HBMs before (black) and after (red) oxygen reduction. **Bd** | The approaching (black) and retracting (red) force—distance curve as well as an AFM image (inset) of an HBM. c.p.s., counts per second; OCP, open circuit potential; ORR, oxygen reduction reaction. Part **Ba** reprinted with permission from REE. <sup>51</sup>, Elsevier. Parts **Bb** and **Bd** adapted with permission from REE. <sup>95</sup>, Elsevier. Part **Bc** reprinted from REE. <sup>25</sup>, Springer Nature Limited.



The phospholipid 1,2-dimyristoyl-sn-glycerol-3-phosphocholine (DMPC) was used to cover the SAM catalyst in a lipid monolayer to form an HBM that is active towards ORR. 1-Dodecanoic acid (DDA) incorporated in the lipid layer was found to enhance the ORR activity of the HBM-embedded porphyrin. This work showcased the opportunity to study and augment molecular catalysts in biomimetic hydrophobic environments.

A dinuclear Cu complex (CuBTT)-based SAM was developed for further ORR studies<sup>18</sup> (FIG. 5b). Here, 1-dodecylboronic acid (DBA) was a pH-dependent proton carrier that delivered protons across the lipid membranes via flip-flop diffusion to boost the ORR activity of CuBTT in the pH 5–7 range<sup>22</sup>. Furthermore, after incorporation of DBA as a proton carrier in the lipid, a linear sweep voltammogram was recorded. An increase

▼ Fig. 5 | Application of HBM platforms towards electrocatalysis. a | Steering the oxygen reduction reaction (ORR) towards the 4e<sup>-</sup> pathway. The structure in red is 1,2-dimyristoyl-sn-glycerol-3-phosphocholine (DMPC). The structure in black is 1-decanethiol. Catalytic amounts of decanoic acid (which acts as a proton carrier) are added to a hybrid bilayer membrane (HBM) that contains an iron-porphyrin catalyst (left). The green arrow indicates the proton flux, and the yellow arrow indicates the electron flow. Electrochemical data are shown on the right 18,22,36. The error bars represent the standard errors in the number of electrons consumed per  $O_2$ . **b** | Transmembrane proton delivery in HBMs can be turned on under acidic conditions by incorporating mono-N-dodecylphosphate (MDP) and 1-dodecylboronic acid (DBA), and under alkaline conditions by embedding tridecanenitrile (TCN). Molecular structures of the protontransfer agents are shown on the left, and their pH-dependence is shown on the right. c | Achieving ORR turnover frequency (TOF) enhancement through shortening the self-assembled monolayer (SAM) length in an HBM. The error bars shown represent the standard errors in the measured cathodic currents. d | Using HBMs to regulate the Faradaic efficiency for CO<sub>2</sub>RR and HER as well as the product selectivity for HCOOH, CO, and  $H_2$ . BTA, benzyl triazole alkyne. Parts **a** to **d** were drawn from data in REFS. <sup>13,18,22,36,74</sup> and REF.  $^{23}$ , respectively. Part  ${\bf a}$  adapted with permission from REF.  $^{13}$ , ACS. Part  ${\bf c}$  adapted with permission from REF.<sup>23</sup>, Wiley. Part **d** is adapted from REF.<sup>74</sup> CC BY 4.0 (https:// creativecommons.org/licenses/by/4.0/).

in the CuBTT catalytic current density was observed here without substantially altering the onset potential for catalysis. This indicates that the proton carrier enhances the kinetics of the ORR without altering the thermodynamics of the reaction. The proton-transfer kinetics to the catalyst was further modulated by changing the concentration of proton carrier in the lipid layer.

Later, kinetic isotope effect studies coupled with a mathematic model and a custom spectroelectrochemical assay were developed to unravel the origin of ORR activity and selectivity optimization  $^{22,171}$ . The extensive study showed that CuBTT undergoes a mixed  $2e^-/2H^+$  and  $4e^-/4H^+$  pathway to generate  $H_2O_2$  as an unwanted byproduct when the proton kinetics are unregulated. Upon restricting proton availability, CuBTT undergoes a  $1e^-/0H^+$  pathway to generate deleterious superoxide. It is only when proton- and electron-transfer rates are comparable that CuBTT undergoes a pure  $4e^-/4H^+$  pathway to generate water as the only desired product with high selectivity. This study highlights the importance of proton transfer kinetics in governing the redox mechanism and product selectivity of PCET reactions  $^{22}$ .

Recently, an HBM was used to study the control of proton and electron transfer to a non-precious-metal Cu ORR catalyst<sup>23</sup> (FIG. 5c). The ORR catalyst, a Cu complex of benzyl triazole alkyne (BTA), was prepared through azide-alkyne click chemistry and covalently attached to the Au electrode through thiol-linked SAMs of different chain lengths. The ORR activity of the CuBTA catalyst with different chain lengths of the SAM covered by a monolayer of DMPC with or without the DBA proton carrier was evaluated. First, the ORR activity of the CuBTA decreases substantially when the SAM is covered by the lipid. The decrease in catalytic activity results from the impeded proton transfer across the lipid membrane.

The electron transfer kinetics to the catalyst was modified by using SAMs with different alkyl chain lengths<sup>23</sup>. Laviron analysis showed that the electron transfer of a longer ( $C_{11}$ ) SAM is 30 times slower than the shorter ( $C_5$ ) SAM. In a manner similar to the modulation of proton transfer kinetics, the onset potential for ORR using  $C_5$  and  $C_{11}$  SAMs does not change substantially.

This observation indicates that the ORR thermodynamics do not change by adjusting the SAM length. However, the reaction kinetics, as reflected by the peak current density, is much less for the  $C_{11}$  SAM than the  $C_5$  SAM because electrons must tunnel through a longer path to reach the catalytic sites. Having established that both the kinetics of proton and electron transfer to the catalyst could be altered using the HBM platform, the effect of the ratio of the proton- and electron-transfer rates  $(k_{\rm H+}/k_{\rm e-})$  on catalyst activity was evaluated. Interestingly, regardless of the SAM used, the ORR current density of the catalyst was directly related to  $k_{\rm H+}/k_{\rm e-}$ . Therefore, the current density of the lipid-covered catalyst can be boosted without altering its core molecular structure, but by tuning the relative rates of proton and electron transfer<sup>23</sup>.

The selectivity of an ORR catalyst can be controlled using the HBM platform of a thiol-based SAM on Au<sup>23</sup>. However, similar platforms are not suitable to control the selectivity of other catalytic systems, such as CO<sub>2</sub> reduction. The thiol-based SAMs on Au are not stable at highly negative potentials, which are required for the CO<sub>2</sub> reduction reaction. Future HBM platforms studying CO<sub>2</sub> reduction could be designed in tandem with recently developed SAMs of porphyrin catalysts using phosphates on metal oxides<sup>172</sup>.

To overcome the problem of the reductive instability of alkylthiol SAMs, a membrane-modified electrochemical platform was developed to control O<sub>2</sub> and CO<sub>3</sub> reduction reaction selectivity<sup>74</sup>. Specifically, two different triazole molecules with different functional groups were synthesized. The ORR catalyst, a dinuclear Cu complex with triazole-based ligands, was covalently attached to Au electrodes through thiol-terminated SAM. An analogous amine-terminated triazole allowed the molecule to attach onto a carbon substrate. In both cases, DMPC lipid layers with or without proton carriers were formed on top of the SAMs. Importantly, the O<sub>2</sub> reduction on carbon substrate was similar to what was observed on membrane-modified Au substrates<sup>74</sup>. In designing active catalysts, this finding suggests that carbon and Au HBMs can be equally effective.

Carbon HBMs with their wider electrochemical windows have been used to study the CO2 reduction reaction. Specifically, a Ag triazole complex has been constructed on a carbon HBM to catalyse the reduction of CO<sub>2</sub> (REF.<sup>74</sup>) (FIG. 5d). Membrane-modified carbon electrodes were used to evaluate CO2 reduction under varying proton transfer rates. The reduction of CO<sub>2</sub> could take place through three different competing pathways: slow proton transfer with the Ag triazole catalyst covered by a lipid monolayer and generating oxalate; regulated proton transfer with the catalyst covered by a membrane with proton carriers to produce either CO or HCOOH, depending on the nature of the catalyst used; and fast proton transfer with the catalyst exposed directly to the aqueous solution to generate H2. The relative rates to produce H2, CO, and HCOOH can be controlled via proton-transfer kinetics across the lipid membrane.

An electrode containing the Ag triazole complex without the lipid membrane produces about the same amount of CO and HCOOH (15% Faradaic efficiency) and a substantial amount of  $\mathrm{H}_2$ . Covering the catalyst

#### Laviron analysis

A mathematical method of determining the electron transfer rate constant of redox-active species adsorbed on an electrode by varying the scan rate in cyclic voltammetry.

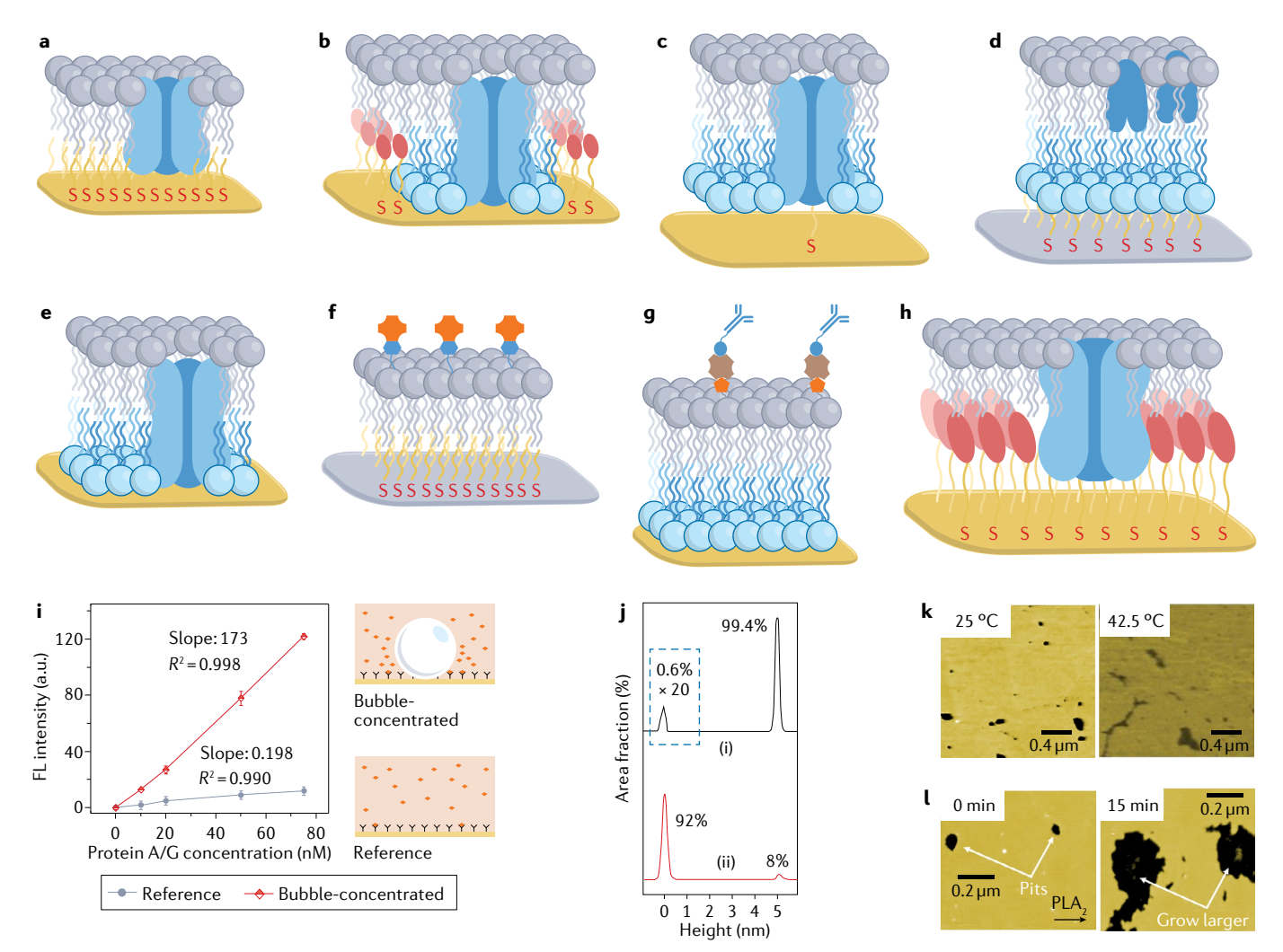


Fig. 6 | **Application of HBM platforms towards biomimicry. a** | A hybrid bilayer membrane (HBM) with a rigid alkanethiol underlayer to study enzymatic activity<sup>181</sup>. **b** | An HBM with a mixed self-assembled monolayer (SAM) with diluent to anchor a lipid bilayer to evaluate transmembrane activity<sup>181</sup>. **c** | An HBM with the membrane protein of interest immobilized to the surface via covalent linkage<sup>181</sup>. **d** | An HBM containing cholesterol oxidase with the bottom leaflet of the lipid bilayer tethered onto the surface<sup>173</sup>. **e** | An HBM with unique lipid compositions in the top and bottom leaflets<sup>181</sup>. **f** | An avidin–biotin HBM for biosensing<sup>103</sup>. **g** | A streptavidin–biotin HBM functionalized with the lgG antibody for antigen recognition. **h** | Biosensing performance of an HBM-based platform. **i** | An HBM with gramicidin A channels on Au electrodes for surface-enhanced infrared absorption spectroscopy (SEIRAS)<sup>186</sup>.

Protein A/G, a genetically engineered recombinant fusion protein between protein A and protein G, displaying the combined binding profiles of IgG antibodies.  $\bf j$  | Atomic force microscopy (AFM) height profile differences before and after addition of PLA $_2$  to an HBM. The percentages refer to the free area of dipalmitoylphosphatidylcholine (DPPC) bilayer after adding phospholipase A $_2$  (PLA $_2$ ) to the HBM system.  $\bf k$  | AFM images of a supported DPPC bilayer obtained at 25 °C (left) and 42.5 °C (right) in a Tris-buffer solution containing 5 mM Ca $^{2+}$ . The size of AFM images is 2  $\mu$ m × 2  $\mu$ m.  $\bf l$  | In situ AFM images of a supported DPPC bilayer acquired before (left) and after (right) the injection of PLA $_2$  at 25 °C. FL, fluorescence. Parts  $\bf g$  and  $\bf i$  adapted with permission from REF. <sup>188</sup>, ACS. Parts  $\bf j$  and  $\bf l$  adapted with permission from REF. <sup>198</sup>, Elsevier. Part  $\bf k$  adapted with permission from REF. <sup>197</sup>, RSC.

with a lipid layer decreases the production of  $\rm H_2$  from 71% to 56%<sup>74</sup>. The decrease in  $\rm H_2$  production is thought to result from the hydrophobic nature of the lipid impeding proton transfer to the catalyst. As a result of this impeded proton transfer, the catalyst has relatively more time to bind and reduce  $\rm CO_2$  to either CO (32%) or HCOOH (12%). Furthermore, the production of  $\rm H_2$  increases from 56% to 77% when a proton carrier is added to the lipid layer. The proton carrier enhances proton-transfer kinetics to the catalyst, which results in the increase of  $\rm H_2$  production. Interestingly, the ratio of CO to HCOOH produced increases in the presence of proton carriers as well, but the origin of this change in product selectivity is unclear  $\rm ^{74}$ .

Biological system modelling. Redox proteins and enzymes involved in biological energy conversion processes often reside in two-dimensional bilayer membranes that contain lipids and cholesterols<sup>173-175</sup>. Various methods have been developed to immobilize these proteins onto surfaces, such as metal-affinity methods using histidine tags<sup>176</sup>, and trapping in surfactants<sup>177,178</sup>. Electrode-supported HBMs provide a unique biocompatible platform with in-vivo-like properties to study redox proteins, enzymes and channels<sup>179</sup>. Here we present a few diverse examples of the applications of HBMs in biology<sup>180,181</sup> (FIC. 6).

One of the first investigations of enzymatic activity and signal/charge transport using HBMs was carried

#### Michaelis constant

 $(K_m)$ . Measures the affinity between the transporter and its substrate.  $K_m$  is defined as the substrate concentration that is transported at half the maximum velocity.

#### Quartz crystal microbalance Records the change in frequency of a quartz crystal resonator to measure the mass

variation per unit area for determining the surface affinity of molecules in liquid.

#### Marangoni convection

A physical phenomenon driven by the surface tension gradient on the surface of a thin liquid

out by evaluating the interaction of isoprenoid ubiquinone with the enzyme pyruvate oxidase<sup>182</sup>. Ubiquinone is an essential component of physiological membranes because it allows communication between enzyme complexes in many of the electron-transport chain steps<sup>183</sup>. These studies utilized an HBM of DMPC on octadecyl silane monolayer on porous aluminium oxide on a Au electrode<sup>182,183</sup> (FIG. 6a). Ubiquinone was incorporated into an HBM during vesicle formation, and pyruvate oxidase was reconstituted into the HBM after its formation. The pyruvate-oxidized ubiquinone diffuses through the two-dimensional matrix to the electrode surface where it is regenerated. The reported Michaelis constant ( $K_m$ ) 1.8 ± 0.7 pmol cm<sup>-2</sup> is very close to the known natural quinone concentration in bacterial membranes. On the other hand, the  $K_m$  values obtained in aqueous three-dimensional matrix differ noticeably.

Although peripheral enzymes like pyruvate oxidase can be easily studied using HBMs, the rigidity of the underlying SAM leaflet inhibits the study of many membrane-bound enzymes and channels that require flexibility and space in both leaflets of the membrane. To address this limitation, the first direct electrochemical response between electrode and the enzyme was reported using fused vesicles were reconstituted with cytochrome c oxidase on top of a controlled submonolayer of octadecyl thiol<sup>184</sup> (FIG. 6b). This construct was then used to measure the rate of electron transfer from cytochrome c to cytochrome c oxidase. To date, cytochrome c oxidase remains one of the most-studied membrane-bound redox enzymes on electrode-supported HBMs<sup>180,181</sup>.

Tethered bilayer membranes use synthetic thiol-modified lipids in place of alkane thiols 180,181 (FIG. 6c). These lipid-thiols can resemble the native bilayer environment more closely and allow for more flexibility in the anchoring leaflet, while maintaining a high level of stability<sup>52</sup>. Tethered bilayer lipid membranes were co-adsorbed with cholesterol oxidases and 1,2-dioleoyl-sn-glycero-3-phosphoethanolamine (DOPE) on a monolayer of 1,2-diphosphothioethanol on tin-doped indium oxide (ITO) using an electrochemical flow chamber  $^{173}$  (FIG. 6d).  $H_2O_2$  was then measured amperometrically at the ITO surface as the by-product of oxidation of cholesterol to cholestenone. This methodology was applied to the functionalization of a Pt microelectrode, which was used to measure cholesterol in live cells. The transport of cholesterol to the plasma membrane from storage compartments inside the cell could be tracked using this approach<sup>173</sup>.

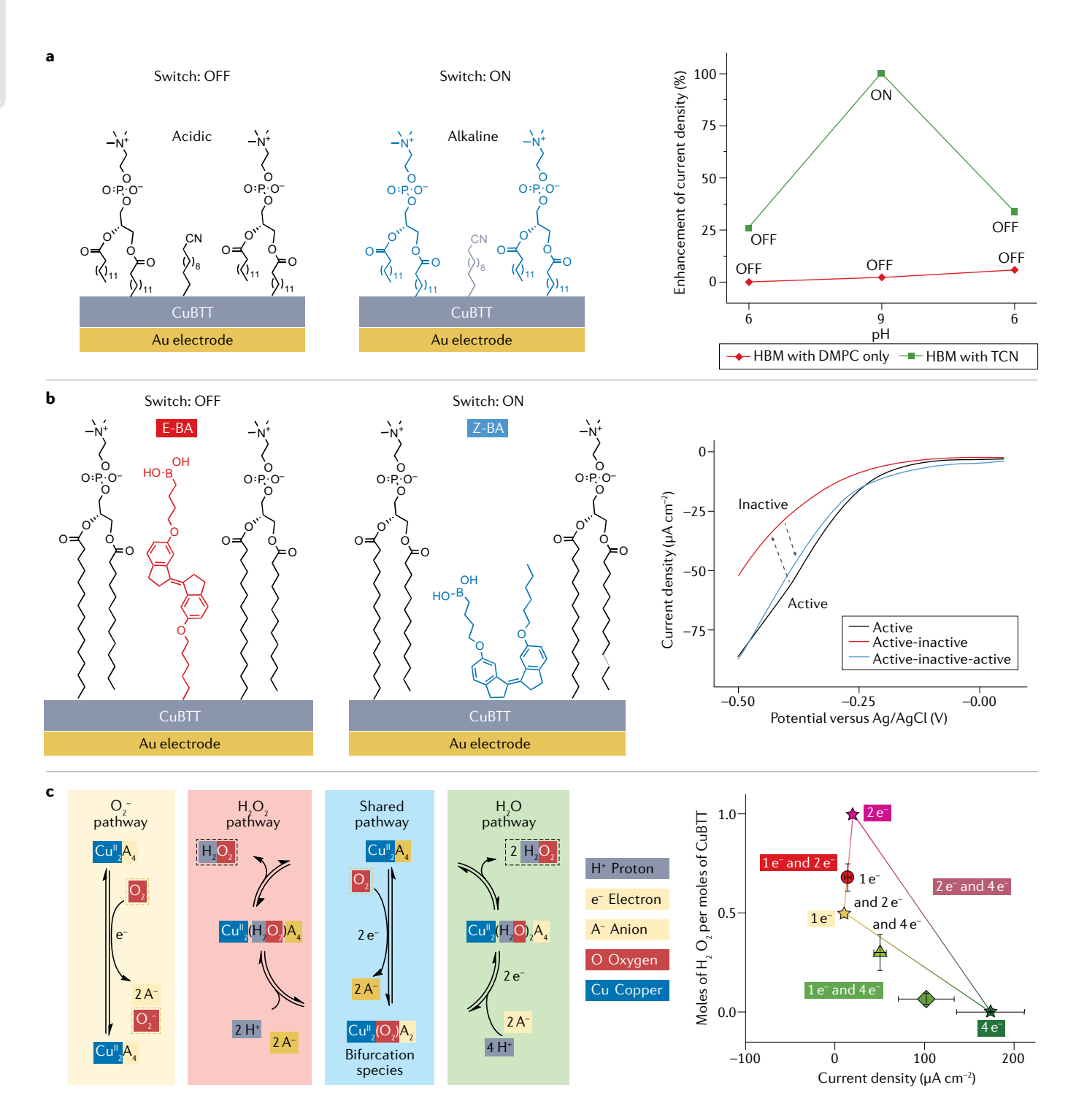
More recently, the application of HBMs to understand membrane activity has been extended to channels<sup>102,185</sup> (FIG. 6e). For example, the selectivity of gramicidin towards monovalent and divalent cations has been evaluated using impedance spectroscopy<sup>186</sup>. Metabolism and photosynthesis are complex membrane processes and with increased understanding of tethered bilayers, enzymes and channels, the complexity of HBM systems has increased to allow for analysing DNA-lipid hybrids<sup>187</sup>, lipid nanoassemblies<sup>75</sup>, protein complexes<sup>188</sup> and cells on solid electrode supports<sup>59</sup>.

Beyond the fundamental study of membrane enzymes and channels, HBMs offer a convenient tool for the

preparation of functionalized sensor surfaces (FIG. 6f). The crystallinity and density of the underlying SAM can now help to enhance stability and longevity. They have been shown to be stable under flow conditions, have low affinity for nonspecific binding, and allow for the regeneration of the underlying monolayer. HBMs offer controlled orientation and dispersion of capture agents, which can be incorporated by reconstituting the vesicles or during vesicle formation. Immobilization on solid supports allows for the use of a wide range of transduction methods<sup>111</sup>. The efficiency of detecting the immunoglobulin G antibody incorporated into HBMs was compared with traditional chemical surface modification using quartz crystal microbalance (FIG. 6g). Biotin was attached to a mixed monolayer of 11-mercaptoundecanoic acid and 6-mercapto-1-hexanol using diimide-mediated coupling (with 1-ethyl-3-(3-dimethylaminopropyl)carbodiimide (EDC) and N-hydroxysuccinimide (NHS)), while biotin was incorporated into HBMs at the vesicle-preparation step. Although the HBM system presented similar efficiency to that of traditional monolayer attachment, the reproducibility and ease of preparation of HBMs in the absence of chemical transformation are advantageous. In a similar study, an avidin-incorporated HBM was used as a label-free DNA biosensor that can be easily regenerated<sup>79,103</sup>. Interestingly, in this report a higher sensitivity was observed for the HBM platform when compared to a traditional EDC/NHS coupled surface<sup>78</sup> (FIG. 6h). This avidin-tethered HBM on Au nano-islands was used to demonstrate the advantage of low-power bubble generation, which can be used for an in situ concentrator by inducing Marangoni convection<sup>189</sup>. The zwitterionic nature of the lipid stabilizes the perfluoropropane (PFP) bubbles on the surface, where the induced Marangoni convection has increased the response time by a factor of 30 and sensitivity by an order of magnitude when compared to a standard diffusion-limited setting<sup>78</sup>.

The first application of HBMs reported as sensing platforms involved the use of SPR to understand the specific binding of profilin to PIP- and PIP2-modified lipids<sup>111</sup>. HBMs have been further examined using surface-enhanced infrared absorption spectroscopy (SEIRAS) and EIS186 (FIG. 6i). Also, the mobility of the receptors in the lipid layer, similar to that of natural systems, was considered to be beneficial for self-optimization towards analyte capture, which is not possible by covalent immobilization. HBMs were designed to establish the lipid permeability parameter of molecular anions<sup>56</sup>. Using factorial analysis, the basicity and dipole moment of anions were deduced to be key attributes that dictate the lipid permeability parameter of anions. Therefore, such an HBM platform can be used to understand the key factors that determine the lipid-crossing ability of anionic, cationic and neutral drug molecules that are important to disease diagnosis and treatment.

Beyond sensing applications, supported HBMs can be used to investigate the melting temperature  $(T_m)$  of lipid bilayers, the value at which lipid bilayer changes from the gel phase (rigid) to the liquid phase (mobile)190. AFM and SFG were used to examine the phase-transition process of supported HBMs. The AFG and SFG results



Mica

A freshly cleaved mica plate can be used in AFM studies owing to its surface flatness at the atomic level. allow for the understanding of how collective lipid motions and membrane fluidity can dictate the activities of membrane-bound enzymes, self-diffusion and the flip-flop processes of lipids  $^{191-195}$ . AFM studies showed that the top leaflet of a dipalmitoylphosphatidylcholine (DPPC) bilayer supported on mica undergoes phase transition at the  $T_{\rm m}$ , while the bottom leaflet adjacent to the substrate reaches the liquid phase at a temperature higher than  $T_{\rm m}$  (REE.  $^{107}$ ) (FIG. 6j). This phenomenon was attributed to the strong interaction between the substrate and the bottom leaflet. SFG results for an asymmetric DPPC-d75/DPPC bilayer showed that the asymmetric

ordering of the supported HBM decreases owing to an increase in the rate of flip-flop diffusion during the heating process<sup>107</sup>.

HBMs have also been designed to understand how the physical state of supported bilayers alters enzymatic activities (FIG. 6k). Phospholipase  $A_2$  (PLA<sub>2</sub>) was found to display enhanced activity at a  $T_{\rm m}$  value in the range of phospholipids on supported HBMs<sup>196,197</sup>. Using AFM, PLA<sub>2</sub> was found to initiate the hydrolysis of the supported DPPC bilayer at the edge of pits present on the HBM<sup>198</sup> (FIG. 6l). The topography and friction of saturated 1,2-distearoyl-sn-glycero-3-phosphorylethanolamine

 Fig. 7 | Application of HBM platforms towards molecular switches. a | Tridecanenitrile (TCN) (left) is a proton gate that can be activated in a base. Upon switching from pH 6 to pH 9, the activity of a hybrid bilayer membrane (HBM)-embedded catalyst is enhanced (right). The electrocatalyst can then be turned off by switching from pH 9 back to pH 6. **b** A photon-triggered proton switch (left) can be realized in an HBM. Electrochemical data (right) demonstrate that upon 390-nm illumination and 360-nm irradiation, an HBM electrocatalyst can be turned off and on, respectively, without altering the pH of the system. c | Proton-coupled electron transfer (PCET) pathway switching by balancing the kinetics of the proton and electron transfer steps. Slow proton transfer leads to 1e<sup>-</sup> pathway, resulting in O<sub>2</sub><sup>-</sup> formation (yellow panel). An initial shared 2e<sup>-</sup> pathway leads to a bifurcation species (blue panel). Under fast proton-transfer conditions, the O, adduct is protonated off as H<sub>2</sub>O<sub>2</sub> (red panel). With optimal proton and electron transfer rates,  $\rm H_2O$  is generated exclusively as the desired  $4e^-$  reduction product (green panel). The triangular plot on the right depicts the relationship between the amount of H<sub>2</sub>O<sub>2</sub> detected and the PCET pathway undergone by the catalyst. The yellow, red and green stars represent the pure 1e<sup>-</sup>, 2e<sup>-</sup> and 4e<sup>-</sup> pathways, respectively. The lines between the stars represent mixtures of two pathways. The triangular space bound by the three stars (vertices) encompasses possible mixtures of all three PCET pathways. The vertical error bars represent the standard errors in the number of moles of H<sub>2</sub>O<sub>2</sub> generated, and the horizontal error bars represent the standard errors in the measured current density. BTT, 6-((3-(benzylamino)-1,2,4-triazol-5-yl)amino)hexane-1-thiol; DMPC, 1,2-dimyristoylsn-glycerol-3-phosphocholine; E-BA, (E)-(4-((6'-(hexyloxy)-2,2',3,3'-tetrahydro-[1,1'-biindenylidene]-6-yl)oxy)butyl)boronic acid; Z-BA, (Z)-(4-((6'-(hexyloxy)-2,2',3,3'tetrahydro-[1,1'-biindenylidene]-6-yl)oxy)butyl)boronic acid. Parts a and b adapted with permission from REF.36 and REF.94, respectively, ACS. Part c adapted from REF.22, Springer Nature Limited.

> (DSPE) and unsaturated 1,2-dioleoyl-sn-glycero-3-phosphoethanolamine (DOPE) supported HBMs were determined using AFM199. DSPE/DOPE HBMs display a DSPE-rich gel-phase domain and a DOPE-rich liquid-phase domain at room temperature, suggesting that lipid phase separation and domain formation can be obtained on biomimetic supported lipid bilayers. The interface between the coexisting liquid-phase and gel-phase domains could act as a preferential site for PLA<sub>2</sub>-catalysed hydrolysis<sup>196,200</sup>. Compared to flat lipid bilayers, the ripple phase with a corrugated structure and well defined periodicity represents an intriguing surface morphology<sup>201,202</sup>. The local spontaneous curvature can be observed in supported double bilayers when the interaction between the substrate and the second bilayer is suppressed<sup>203</sup>. The ripple phase exhibits a higher sensitivity to enzymatic reaction, while PLA, preferentially hydrolyses DMPC in DMPC/DSPC ripples<sup>204</sup>. These AFM results suggest that lipid domains, bilayer structures and membrane components of HBMs can control the substrate preference and reactivity of enzymes.

> Smart materials and molecular devices. HBM platforms can also exhibit functions beyond electrocatalysis and biomimicry. A Cu-complex-based HBM with a lipid layer containing mono-N-dodecylphosphate (MDP) was used to build a prototypical pH-dependent proton switch<sup>18</sup>. In its neutral form, MDP exists in an off state in which the molecule is too hydrophilic to penetrate the hydrophobic portion of the lipid layer<sup>95</sup>. Upon acidification, MDP can access the uncharged on state, which can deliver protons across the membrane to activate an HBM-embedded catalyst. This phosphate-based proton switch undergoes a flip-flop transmembrane mechanism and can be turned off upon basification<sup>15</sup>.

Further demonstrating the utility of an HBM as a protonic device, a base-activated HBM with a bio-inspired

proton gate designed on the basis of naturally occurring protonophores was developed<sup>36</sup> (FIG. 7a). Instead of using bound protons, this nitrile proton switch uses hydrogen-bonded water to turn on the activity of a lipid-buried ORR catalyst under an alkaline environment. Through this mechanism, this tridecanenitrile (TCN) could allow for the construction of future molecular circuits that can be switched on in base and switched off in neutral conditions. In the future, advanced bioprotonic devices could be developed by coupling MDP with TCN or other designer molecules. Beyond taking advantage of the pH difference to induce proton delivery, a photoswitch with a response time of less than 5 seconds has been developed to trigger transmembrane proton transfer in an HBM system94 (FIG. 7b). A photoisomerizable stiff stilbene unit was incorporated in the middle of a proton switch equipped with a terminal boronic acid head group to enable on-demand proton delivery. This photo-controlled on-off behaviour has potential for developing photoprotonic devices.

In addition to turning on and off catalytic activity, HBMs can also be engineered to alter electrochemical pathways through regulating the proton transfer rate<sup>22</sup> (FIG. 7c). For instance, the PCET pathways of an HBM-bound quinone — installed at the SAM-lipid interface of an HBM — can be altered73. When the quinone moiety has free access to protons in the bulk solution, a 2e<sup>-</sup>/1H<sup>+</sup> pathway is in operation. The quinone moiety undergoes a 1e<sup>-</sup>/0H<sup>+</sup> pathway under a proton-deprived environment, such as that of a lipid membrane. Upon the incorporation of a proton regulator, the quinone switches to a sequential pathway with a 1e<sup>-</sup>/1H<sup>+</sup> step followed by another 1e<sup>-</sup>/1H<sup>+</sup> step. HBMs can also be used to distinguish anions present in solution for smart applications<sup>56</sup> (FIG. 8a). These pioneering efforts open up new avenues towards precision steering of redox reaction mechanisms and the development of smart materials with pre-programmed functions.

To complete the circuit for a nanoscale device, HBMs have been designed to facilitate oxidation reactions in addition to the aforementioned reduction reactions. A ferrocene-embedded HBM was demonstrated to oxidize ascorbic acid, thereby allowing the possibility to use ascorbic acid as the fuel for self-propelling HBM nanoparticles  $^{21}$  (FIG. 8b). Recently, a carbon-supported HBM with a Ru complex that allows for controllable oxidation of  $\rm H_2O_2$  was developed, further adding one more fuel choice to HBM-based nanomachines  $^{205}$  (FIG. 8c). In short, HBMs have bright prospects in designing next-generation stimuli-responsive sensing technologies with collective intelligence for real-time diagnosis and self-powered surveillance under practical conditions and physiological environments.

#### **Future challenges**

Overall platform stability. Current HBM systems mostly use single-component DMPC on nominally flat surfaces, because DMPC is the major component of the mitochondrial membrane<sup>206</sup>. These structures are an oversimplification of the native lipid membrane environment. The library of HBMs could be expanded by a systematic increase in component complexity inspired

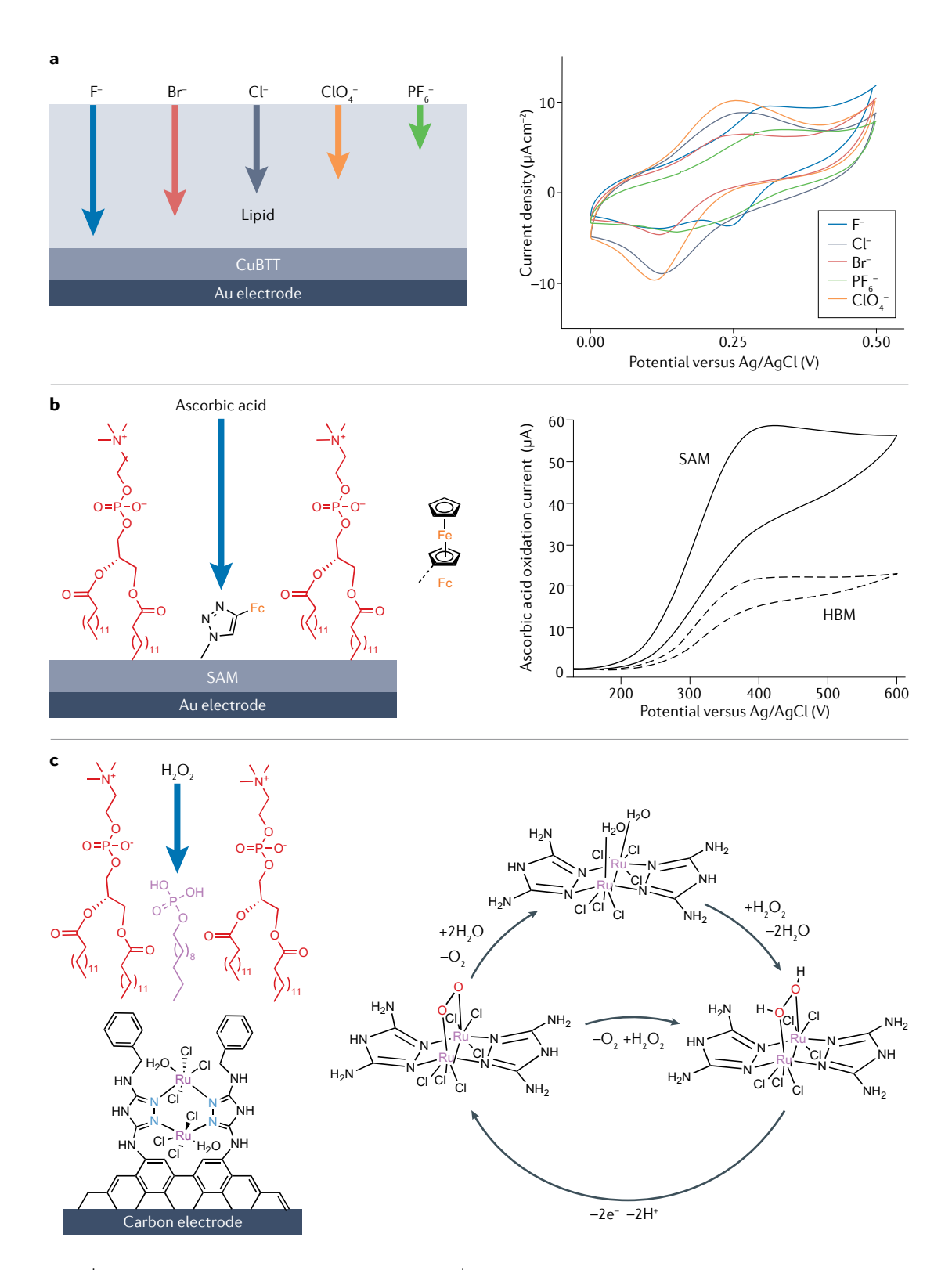


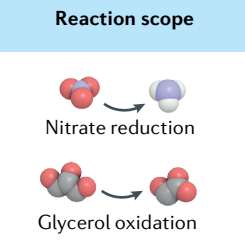
Fig. 8 | Application of HBM platforms towards sensors. a | Assessing anion transmembrane permeability using a CuBTT hybrid bilayer membrane (HBM) (left). Cyclic voltammograms (CVs) of HBMs in pH 5 solution containing 100 mM KCl (black), KBr (red), KF (blue), KPF $_6$  (green) and KClO $_4$  (orange) at a scan rate of 100 mV s $^{-1}$ , and the midpoint potential ( $E_{1/2}$ ) and peak-to-peak potential separation ( $\Delta E_p$ ) observed in the CVs reflect the thermodynamics and kinetics of anion transport through HBMs. **b** | Ascorbic acid quantification using a ferrocene (Fc) self-assembled monolayer (SAM) and its corresponding HBM with their structures shown on the left and their CVs shown on the right (the solid line indicates the SAM, and the dashed line indicates the HBM). **c** |  $H_2O_2$  detection using a RuBTA HBM with its structure shown on the left. The proposed  $H_2O_2$  oxidation pathway enabled by RuDAT is shown on the right. BTA,  $N^5$ -benzyl-1H-1,2,4-triazole-3,5-diamine; BTT: 6-((3-(benzylamino)-1,2,4-triazol-5-yl)amino)hexane-1-thiol; DAT, 3,5-diamino-1,2,4-triazole. Parts **a** to **c** were drawn from data in REFS. 21.56 and 205, respectively. Parts **a**-**c** adapted with permission from REF.56, REF.21 and REF.205, respectively.

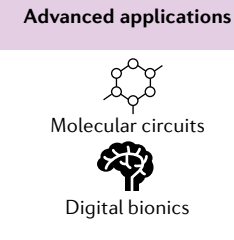
# Platform stability pH range Surface functionalization

# Transmembrane delivery Lipid Artificial

channels

complexity





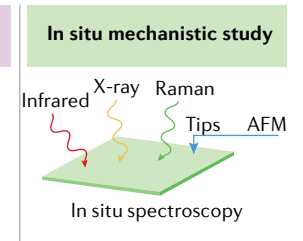


Fig. 9 | A roadmap presenting future research directions for HBMs. Exploiting the versatility of hybrid bilayer membrane (HBM) modules to tackle pressing issues in biomimicry and proton-coupled electron transfer (PCET) catalysis that have broad implications in understanding biological systems and realizing renewable energy schemes. AFM, atomic force microscopy.

by natural systems. This effort could reveal differences in the functionality of each component from diverse origins (bacterial versus mammalian) or cells in different states (cancerous versus non-cancerous). In natural systems, the appropriate curvatures of different membranes have critical roles in regulating membrane properties and functions<sup>207</sup>. The construction and study of HBMs on both concave and convex surfaces that match the biological system is a natural next step to diversify and expand the study of membrane functions. The classes of HBM may also be expanded to include other surface-modification chemistries, depending on analytical needs. For example, an oxide-phosphate on a glass or TiO, substrate could provide transparency for optical measurements and carbon grafting could provide additional mechanical stability together with desirable electrical conductivity.

Transmembrane delivery mode. Proton delivery in HBMs has been achieved by flip-flop diffusion of mixtures of proton transfer agents and lipids, and the kinetics of proton transfer have been tuned by the ratio of these two components. Although this approach has provided important insights into the mechanism of PCET reactions, it relies on the homogeneous distribution of the proton carriers in the lipid, which may not be attainable in all systems. The covalent attachment of proton carriers and artificial ion channels to the catalyst through synthetic schemes could overcome this limitation and broaden the scope of proton transfer agents that can be incorporated into the lipid layer of HBMs. Such covalent incorporation of proton carriers could allow them to be appended near a buried electrocatalyst, which could enhance catalyst proton transfer kinetics. These covalently attached proton transfer agents could include amino acids that more accurately mimic biological peptide-based proton channels. One other limitation of current studies is the amphiphilic nature of proton carriers, which can lead to their dissolution in the bulk environment and thus loss of functionality. To minimize this effect, proton carriers can be designed with mechanical interlocking systems using additional supramolecular interactions to provide more robust platforms for multi-cycle regulation of HBM functions.

**Reaction scope.** At present, HBMs have only been utilized to overcome activity–selectivity dilemmas in electrocatalytic processes with up to four PCET steps, such

as ORR. HBMs are anticipated to fill the next knowledge gap in even more complex reactions involving more than four PCET steps. These complex reactions include the reduction of nitrate and nitrite in waste-to-commodity conversion as well as the oxidation of glycerol and ethylene glycol for feedstock upcycling. By modulating the membrane environment, HBMs have the potential to alter reaction pathways via the changing favourability of intermediates and controlling the retention time of bound adducts. Upon coupling light-driven redox catalysis with downstream thermal reactions at the unique membrane–SAM interface, HBMs are envisioned to optimize the photon–electron–proton interplay to further transform high-energy transient species into value-added products exclusively.

In situ mechanistic studies. Previously, the PCET mechanism on HBMs was inferred from indirect kinetic isotope effect and Tafel slope analyses. Taking advantage of the component modularity of HBMs, HBMs can be deposited on substrates tailored to various spectroscopic methods. With the advent of in situ spectroscopic techniques, the sensing mechanism, adduct formation and reaction progression on HBMs can be monitored via X-ray absorption, surface-enhanced Raman and infrared, and reflectance UV-visible spectroscopy in real time. For instance, the interactions between oxygen molecules and coordinated metal ions can be interrogated using potential-dependent X-ray absorption and Raman spectroscopy during ORR. The unique mechanistic insights gained through HBMs can feed back to assist the rational design of next-generation bioanalytical devices and energy catalysis systems.

Molecular circuits. The ability to design a pH-sensitive switch to turn electrocatalytic reactions on and off within an HBM platform opens up the possibility of linking multiple HBM electrodes to design more complicated circuits and logic gates. In principle, these circuits could form the basis of a new class of in vivo computational systems. When applied to the selective generation of reactive species, this switching ability of HBMs might also have future biomedical applications. For example, ORR catalysts in HBMs could respond to pH changes in cancer cells and selectively generate partially reduced oxygen species such as superoxides, which can subsequently destroy infected cells.

#### **Conclusions and future directions**

This Review has demonstrated the utility of HBMs. From a knowledge creation standpoint, HBMs have advanced our understanding of PCET processes by providing a framework to delineate the convoluted effects of electron- and proton-transfer thermodynamics and kinetics. Additionally, HBMs allow for the development of structural and functional surrogates of multi-component biological machinery to understand how the components work together in an integrated manner. Apart from learning more about natural systems, HBMs have been applied to practical scenarios to address the challenges associated with exclusive yield of a desired product at high catalytic turnover.

HBMs have the potential to become the next class of smart nanomaterial, with impacts in multiple emerging fields (FIG. 9). In the future, colloidal HBMs with quantum dots as cores are envisioned to regulate the intricate dynamics among electrons, protons and photons for photocatalysis. HBM-decorated coinage-metal

nanoparticles could further enable in situ spectroscopic investigations of transmembrane pathways of molecular drugs as well as bio-relevant entities. Active matter coated with biocompatible HBMs could allow programmable collective motions and executable in vivo actions for disease diagnosis and treatment. In addition to constructing self-powered nanomachines, HBMs could provide precise product selectivity with high yields in multistep organic electrosynthesis of industrial relevance. HBMs could replicate the whole of photosystems I and II to enable next-generation renewable energy schemes. Further expanding the variations of HBMs and combined with cutting-edge real-time characterization technologies, HBMs could be useful in research fields such as molecular devices, real-time reaction monitoring, precise control over catalytic pathways and the complete recapitulation of biological systems.

Published online: 28 October 2022

- Chen, H., Dong, F. & Minteer, S. D. The progress and outlook of bioelectrocatalysis for the production of chemicals, fuels and materials. *Nat. Catal.* 3, 225–244 (2020).
- Morello, G., Megarity, C. F. & Armstrong, F. A. The power of electrified nanoconfinement for energising, controlling and observing long enzyme cascades. *Nat. Commun.* 12, 340 (2021).
- Weliwatte, N. S. & Minteer, S. D. Photobioelectrocatalytic CO<sub>2</sub> reduction for a circular energy landscape. *Joule* 5, 2564–2592 (2021).
- Das, J. et al. Reagentless biomolecular analysis using a molecular pendulum. *Nat. Chem.* 13, 428–434 (2021).
- Saunders, S. H. et al. Extracellular DNA promotes efficient extracellular electron transfer by pyocyanin in *Pseudomonas aeruginosa* biofilms. *Cell* 182, 919–932 (2020).
- Sempionatto, J. R. et al. An epidermal patch for the simultaneous monitoring of haemodynamic and metabolic biomarkers. *Nat. Biomed. Eng.* 5, 737–748 (2021).
- Evans, R. M. et al. The value of enzymes in solar fuels research — efficient electrocatalysts through evolution. *Chem. Soc. Rev.* 48, 2039–2052 (2019).
- Guo, Y., Stroka, J. R., Kandemir, B., Dickerson, C. E. & Bren, K. L. Cobalt metallopeptide electrocatalyst for the selective reduction of nitrite to ammonium. *J. Am. Chem. Soc.* 140, 16888–16892 (2018).
- Le, J. M. & Bren, K. L. Engineered enzymes and bioinspired catalysts for energy conversion. ACS Energy Lett. 4, 2168–2180 (2019).
- Kim, J., Campbell, A. S., de Ávila, B. E.-F. & Wang, J. Wearable biosensors for healthcare monitoring. Nat. Biotechnol. 37, 389–406 (2019).
- Yang, Y. et al. A laser-engraved wearable sensor for sensitive detection of uric acid and tyrosine in sweat. Nat. Biotechnol. 38, 217–224 (2020).
- Ngo, F. M. & Tse, E. C. M. Bioinorganic platforms for sensing, biomimicry, and energy catalysis. *Chem. Lett.* 50, 974–986 (2021).
- 13. Hosseini, A. et al. Hybrid bilayer membrane: a platform to study the role of proton flux on the efficiency of oxygen reduction by a molecular electrocatalyst. J. Am. Chem. Soc. 133, 11100–11102 (2011). This paper showcases an early work in controlling the oxygen reduction performance of an Fe porphyrin through modulating the proton flux through an artificial lipid membrane.
- Krueger, S. et al. Investigation of hybrid bilayer membranes with neutron reflectometry: probing the interactions of melittin. *Langmuir* 17, 511–521 (2001).
- Barile, C. J. et al. The flip-flop diffusion mechanism across lipids in a hybrid bilayer membrane. *Biophys. J.* 110, 2451–2462 (2016).
- Plant, A. L. Self-assembled phospholipid/alkanethiol biomimetic bilayers on gold. *Langmuir* 9, 2764–2767 (1993)
  - This work lays the foundation of HBM electrodes for biomimicry and electrochemistry.

- Silin, V. I. et al. The role of surface free energy on the formation of hybrid bilayer membranes. *J. Am. Chem. Soc.* 124, 14676–14683 (2002).
- Barile, C. J. et al. Proton switch for modulating oxygen reduction by a copper electrocatalyst embedded in a hybrid bilayer membrane. *Nat. Mater.* 13, 619–623 (2014).
  - This work was the first to describe designing a pH-sensitive switch that can turn on and off the oxygen reduction activity of a Cu complex inside an HBM on demand.
- Vockenroth, I. K. et al. Stable insulating tethered bilayer lipid membranes. *Biointerphases* 3, FA68–FA73 (2008).
- Stelzle, M., Weissmueller, G. & Sackmann, E. On the application of supported bilayers as receptive layers for biosensors with electrical detection. J. Phys. Chem. 97, 2974–2981 (1993).
- Hosseini, A. et al. Ferrocene embedded in an electrodesupported hybrid lipid bilayer membrane: a model system for electrocatalysis in a biomimetic environment. *Langmuir* 26, 17674–17678 (2010).
- Tse, E. C. M. et al. Proton transfer dynamics control the mechanism of O<sub>2</sub> reduction by a non-precious metal electrocatalyst. *Nat. Mater.* 15, 754–759 (2016).
  - This work demonstrates for the first time that an HBM oxygen reduction catalyst that intrinsically undergoes a mixture of 2e- and 4e- pathways can be steered toward facilitating the 4e- pathway exclusively through tuning the transmembrane proton transfer kinetics without covalent modifications.
- Gautam, R. P. et al. Controlling proton and electron transfer rates to enhance the activity of an oxygen reduction electrocatalyst. *Angew. Chem. Int. Ed.* 57, 13480–13483 (2018).
  - This pioneering work establishes the simultaneous control of both electron and proton transfer rates in oxygen reduction to achieve precise regulation of electrocatalytic activity and product selectivity without altering the core molecular structure of an HBM construct.
- Paleos, C. M., Sideratou, Z. & Tsiourvas, D. Molecular recognition of complementary liposomes in modeling cell–cell recognition. *ChemBioChem* 2, 305–310 (2001)
- Ma, W. et al. Investigating electron-transfer processes using a biomimetic hybrid bilayer membrane system. *Nat. Protoc.* 8, 439–450 (2013).
  - This landmark paper details the preparation procedure of a trilayer HBM platform with a lipid bilayer membrane appended on top of a self-assembled monolayer.
- Tamm, L. K. & McConnell, H. M. Supported phospholipid bilayers. *Biophys. J.* 47, 105–113 (1985).
   This work is one of the pioneering papers that conceptualizes the idea of HBM.
- Ries, R. S., Choi, H., Blunck, R., Bezanilla, F. & Heath, J. R. Black lipid membranes: visualizing the structure, dynamics, and substrate dependence of

- membranes. J. Phys. Chem. B 108, 16040–16049 (2004).
- Sackmann, E. Supported membranes: scientific and practical applications. Science 271, 43–48 (1996).
- Collman James, P. et al. A cytochrome c oxidase model catalyzes oxygen to water reduction under rate-limiting electron flux. *Science* 315, 1565–1568 (2007).
  - This exemplary work establishes how electron flux can be used to control the oxygen reduction behaviour of an Fe porphyrin that has been attached onto self-assembled monolayers with various electron transfer rates.
- Plant, A. L., Gueguetchkeri, M. & Yap, W. Supported phospholipid/alkanethiol biomimetic membranes: insulating properties. *Biophys. J.* 67, 1126–1133 (1994).
- Collman, J. P. & Boulatov, R. Electrocatalytic O<sub>2</sub> reduction by synthetic analogues of the Heme/Cu site of cytochrome oxidase incorporated in a lipid film. Angew. Chem. Int. Ed. 41, 3487–3489 (2002). This paper is among the first examples to suppress partially reduced oxygen products such as deleterious H<sub>2</sub>O<sub>2</sub> from being produced by an electrocatalyst embedded in a lipid enclosure.
- Anderson, N. A., Richter, L. J., Stephenson, J. C. & Briggman, K. A. Characterization and control of lipid layer fluidity in hybrid bilayer membranes. *J. Am. Chem. Soc.* 129, 2094–2100 (2007).
- Krysinski, P., Moncelli, M. R. & Tadini-Buoninsegni, F. A voltammetric study of monolayers and bilayers self-assembled on metal electrodes. *Electrochim.* Acta 45, 1885–1892 (2000).
- Troiano, J. M. et al. Direct probes of 4nm diameter gold nanoparticles interacting with supported lipid bilayers. J. Phys. Chem. C 119, 534–546 (2015).
- Montal, M. & Mueller, P. Formation of bimolecular membranes from lipid monolayers and a study of their electrical properties. *Proc. Natl Acad. Sci. USA* 69, 3561–3566 (1972).
- Zeng, T., Gautam, R. P., Barile, C. J., Li, Y. & Tse, E. C. M. Nitrile-facilitated proton transfer for enhanced oxygen reduction by hybrid electrocatalysts. ACS Catal. 10, 13149–13155 (2020).
  - This work presents a uniquely designed alkyl-nitrile that can facilitate proton transfer in alkaline conditions, enabling the development of a base-activated switch for use in HBMs.
- Han, X., Wang, L., Qi, B., Yang, X. & Wang, E. A strategy for constructing a hybrid bilayer membrane based on a carbon substrate. *Anal. Chem.* 75, 6566–6570 (2003).
- Su, Z., Leitch, J. J. & Lipkowski, J. Electrodesupported biomimetic membranes: an electrochemical and surface science approach for characterizing biological cell membranes. *Curr. Opin. Electrochem.* 12, 60–72 (2018).
- Sabirovas, T., Valiūnienė, A. & Valincius, G. Hybrid bilayer membranes on metallurgical polished aluminum. Sci. Rep. 11, 9648 (2021).

- Sabirovas, T., Valiūnienė, A., Gabriunaite, I. & Valincius, G. Mixed hybrid bilayer lipid membranes on mechanically polished titanium surface. *Biochim. Biophys. Acta* 1862, 183232 (2020).
- Wang, X., Zhang, Y., Bi, H. & Han, X. Supported lipid bilayer membrane arrays on micro-patterned ITO electrodes. RSC Adv. 6, 72821–72826 (2016).
- Lee, B. K., Lee, H. Y., Kim, P., Suh, K. Y. & Kawai, T. Nanoarrays of tethered lipid bilayer rafts on poly(vinyl alcohol) hydrogels. *Lab Chip* 9, 132–139 (2009).

### This pioneering work describes the formation of HBM on single-walled carbon nanotube transistors for biosensing and molecular recognition.

- Fabre, R. M. & Talham, D. R. Stable supported lipid bilayers on zirconium phosphonate surfaces. *Langmuir* 25, 12644–12652 (2009).
- Su, Z. et al. Electrochemical and PM-IRRAS studies of floating lipid bilayers assembled at the Au(111) electrode pre-modified with a hydrophilic monolayer. J. Electroanal. Chem. 688, 76–85 (2013).
- Su, Z., Ho, D., Merrill, A. R. & Lipkowski, J. In situ electrochemical and PM-IRRAS studies of colicin E1 ion channels in the floating bilayer lipid membrane. *Langmuir* 35, 8452–8459 (2019).
- Quinn, J. G. & O'Kennedy, R. Transduction platforms and biointerfacial design of biosensors for 'real-time' biomolecular interaction analysis. *Anal. Lett.* 32, 1475–1517 (1999).
- Deng, Y. et al. Fluidic and air-stable supported lipid bilayer and cell-mimicking microarrays. *J. Am. Chem. Soc.* **130**, 6267–6271 (2008).
- Castellana, E. T. & Cremer, P. S. Solid supported lipid bilayers: from biophysical studies to sensor design. Surf. Sci. Rep. 61, 429–444 (2006).
- van Weerd, J., Karperien, M. & Jonkheijm, P. Supported lipid bilayers for the generation of dynamic cell–material interfaces. Adv. Healthc. Mater. 4, 2743–2779 (2015).
- Meuse, C. W. et al. Hybrid bilayer membranes in air and water: infrared spectroscopy and neutron reflectivity studies. *Biophys. J.* 74, 1388–1398 (1998).
- Knoll, W. et al. Functional tethered lipid bilayers. Rev. Mol. Biotechnol. 74, 137–158 (2000).
- Sek, S., Xu, S., Chen, M., Szymanski, G. & Lipkowski, J. STM studies of fusion of cholesterol suspensions and mixed 1,2-dimyristoyl-sn-glycero-3-phosphocholine (DMPC)/cholesterol vesicles onto a Au(111) electrode surface. J. Am. Chem. Soc. 130, 5736–5743 (2008).
- Berti, D., Caminati, G. & Baglioni, P. Functional liposomes and supported lipid bilayers: towards the complexity of biological archetypes. *Phys. Chem. Chem. Phys.* 13, 8769–8782 (2011).
- Suraniti, E., Tumolo, T., Baptista, M. S., Livache, T. & Calemczuk, R. Construction of hybrid bilayer membrane (HBM) biochips and characterization of the cooperative binding between cytochrome-c and HBM. *Langmuir* 23, 6835–6842 (2007).
- Tse, E. C. M. et al. Anion transport through lipids in a hybrid bilayer membrane. *Anal. Chem.* 87, 2403–2409 (2015).
- Barnaba, C., Taylor, E. & Brozik, J. A. Dissociation constants of cytochrome P450 2C9/cytochrome P450 reductase complexes in a lipid bilayer membrane depend on NADPH: a single-protein tracking study. J. Am. Chem. Soc. 139, 17923–17934 (2017).
- - This work shows that HBMs can mimic a native lipid environment and reveal the membrane integration process of proteins in the presence of NADPH.
- Phillips, K. S., Kang, K. M., Licata, L. & Allbritton, N. L. Air-stable supported membranes for single-cell cytometry on PDMS microchips. *Lab Chip* 10, 864–870 (2010).
- Zhan, W. & Jiang, K. A modular photocurrent generation system based on phospholipid-assembled fullerenes. *Langmuir* 24, 13258–13261 (2008).
- Jiang, K., Xie, H. & Zhan, W. Photocurrent generation from Ru(bpy)<sub>3</sub><sup>2+</sup> immobilized on phospholipid/alkanethiol hybrid bilayers. *Langmuir* 25, 11129–11136 (2009).
- Kim, S. et al. Plasmonic nanoparticle-interfaced lipid bilayer membranes. Acc. Chem. Res. 52, 2793–2805 (2019).

- Zhou, W. & Burke, P. J. Versatile bottom-up synthesis of tethered bilayer lipid membranes on nanoelectronic biosensor devices. ACS Appl. Mater. Interf. 9, 14618–14632 (2017).
- 64. Favero, G. et al. Glutamate receptor incorporated in a mixed hybrid bilayer lipid membrane array, as a sensing element of a biosensor working under flowing conditions. J. Am. Chem. Soc. 127, 8103–8111 (2005). This work describes the development of HBM arrays embedded with glutamate receptors as flowbased bioelectroanalytical sensors with nanomolar sensitivity.
- Zare, M., Kitt, J. P., Wen, X., Heider, E. C. & Harris, J. M. Hybrid-lipid bilayers induce n-alkyl-chain order in reversed-phase chromatographic surfaces, impacting their shape selectivity for aromatic hydrocarbon partitioning. Anal. Chem. 93, 4118–4125 (2021).
- Kornienko, N. et al. Oxygenic photoreactivity in photosystem II studied by rotating ring disk electrochemistry. J. Am. Chem. Soc. 140, 17923–17931 (2018).
- Young, I. D. et al. Structure of photosystem II and substrate binding at room temperature. *Nature* 540, 453–457 (2016).
- 68. Barile, C. J. et al. Inhibiting platelet-stimulated blood coagulation by inhibition of mitochondrial respiration. Proc. Natl Acad. Sci. USA 109, 2539–2543 (2012). Electrochemical results from this HBM work contribute to the understanding of how heterocycles deter mitochondrial platelet stimulation and subsequently inhibit blood clotting.
- Collman, J. P., Dey, A., Barile, C. J., Ghosh, S. & Decréau, R. A. Inhibition of electrocatalytic O<sub>2</sub> reduction of functional CcO models by competitive, non-competitive, and mixed inhibitors. *Inorg. Chem.* 48, 10528–10534 (2009).
- 70. Ma, W. et al. Reversible redox of NADH and NADat a hybrid lipid bilayer membrane using ubiquinone. J. Am. Chem. Soc. 133, 12366–12369 (2011). This work demonstrates the ability to replicate biological redox cycling of NADH through HBM-bound ubiquinones to mimic the initial stages of respiration.
- Jones, S. M. & Solomon, E. I. Electron transfer and reaction mechanism of laccases. *Cell. Mol. Life Sci.* 72, 869–883 (2015).
- Hakulinen, N. & Rouvinen, J. Three-dimensional structures of laccases. *Cell. Mol. Life Sci.* 72, 857–868 (2015).
- Tse, E. C. M. et al. Proton transfer dynamics dictate quinone speciation at lipid-modified electrodes. Phys. Chem. Phys. 19, 7086–7093 (2017).
- Phys. Chem. Chem. Phys. 19, 7086–7093 (2017).
  Supakul, S. N. & Barile, C. J. Membrane-modified metal triazole complexes for the electrocatalytic reduction of oxygen and carbon dioxide. Front. Chem. 6, 543–550 (2018).
  - This work extends the applicability of HBMs to regulating the proton-coupled electron transfer pathway and product distribution of carbon dioxide reduction.
- Wang, M., Chen, J., Lian, T. & Zhan, W. Mimicking photosynthesis with supercomplexed lipid nanoassemblies: design, performance, and enhancement role of cholesterol. *Langmuir* 32, 7326–7338 (2016).
- Wang, M. & Zhan, W. Mimicking photosynthesis with electrode-supported lipid nanoassemblies. Acc. Chem. Res. 49, 2551–2559 (2016).
- Res. 49, 2551–2559 (2016).
  Xie, H., Jiang, K. & Zhan, W. A modular molecular photovoltaic system based on phospholipid/alkanethiol hybrid bilayers: photocurrent generation and modulation. Phys. Chem. Chem. Phys. 13, 17712–17721 (2011).
- 17712–17721 (2011).
   Kim, Y., Ding, H. & Zheng, Y. Enhancing surface capture and sensing of proteins with low-power optothermal bubbles in a biphasic liquid. *Nano Lett.* 20, 7020–7027 (2020).
  - This work shows that HBM model surfaces can serve as high-fidelity biosensors that capture target proteins under high-velocity fluid flows.
- Kim, S. & Choi, S.-J. A lipid-based method for the preparation of a piezoelectric DNA biosensor. *Anal. Biochem.* 458, 1–3 (2014).
- Anal. Biochem. 458, 1–3 (2014).
   Phillips, K. S., Dong, Y., Carter, D. & Cheng, Q. Stable and fluid ethylphosphocholine membranes in a poly(dimethylsiloxane) microsensor for toxin detection in flooded waters. Anal. Chem. 77, 2960–2965 (2005).
- Phillips, K. S., Kottegoda, S., Kang, K. M., Sims, C. E. & Allbritton, N. L. Separations in poly(dimethylsiloxane) microchips coated with supported bilayer membranes. *Anal. Chem.* 80, 9756–9762 (2008).

- Reimhult, E. & Kumar, K. Membrane biosensor platforms using nano- and microporous supports. *Trends Biotechnol.* 26, 82–89 (2008).
- Alvarez-Malmagro, J. et al. Molecular recognition between guanine and cytosine-functionalized nucleolipid hybrid bilayers supported on gold (111) electrodes. *Bioelectrochemistry* 132, 107416 (2020).
- Gallagher, E. S. et al. Hybrid phospholipid bilayer coatings for separations of cationic proteins in capillary zone electrophoresis. *Electrophoresis* 35, 1099–1105 (2014).
- Podolsky, K. A. & Devaraj, N. K. Synthesis of lipid membranes for artificial cells. *Nat. Rev. Chem.* 5, 676–694 (2021).
- Langton, M. J. Engineering of stimuli-responsive lipidbilayer membranes using supramolecular systems. *Nat. Rev. Chem.* 5, 46–61 (2021).
- Herrmann, I. K., Wood, M. J. A. & Fuhrmann, G. Extracellular vesicles as a next-generation drug delivery platform. *Nat. Nanotechnol.* 16, 748–759 (2021).
- Murphy, D. E. et al. Extracellular vesicle-based therapeutics: natural versus engineered targeting and trafficking. Exp. Mol. Med. 51, 1–12 (2019).
- Brevnov, D. A. & Finklea, H. O. Alternating current voltammetry studies of the effect of melittin on heterogeneous electron transfer across a hybrid bilayer membrane supported on a gold electrode. *Langmuir* 16, 5973–5979 (2000).
- Peng, Z., Tang, J., Han, X., Wang, E. & Dong, S. Formation of a supported hybrid bilayer membrane on gold: a sterically enhanced hydrophobic effect. *Langmuir* 18, 4834–4839 (2002).
- 93. Bain, C. D. et al. Formation of monolayer films by the spontaneous assembly of organic thiols from solution onto gold. *J. Am. Chem. Soc.* **111**, 321–335 (1989).
- Li, Y., Tse, E. C. M., Barile, C. J., Gewirth, A. A. & Zimmerman, S. C. Photoresponsive molecular switch for regulating transmembrane proton-transfer kinetics. *J. Am. Chem. Soc.* 137, 14059–14062 (2015). This work details the development of a light-gated HBM switch that can initiate and stall electrocatalysis in real time, paving the way to turning photo-electro-protonic devices into reality.
   Zeng, T., Wu, H.-L., Li, Y., Tse, E. C. M. & Barile, C. J.
- Zeng, T., Wu, H.-L., Li, Y., Tse, E. C. M. & Barile, C. J. Physical and electrochemical characterization of a Cu-based oxygen reduction electrocatalyst inside and outside a lipid membrane with controlled proton transfer kinetics. *Electrochim. Acta* 320, 134611 (2019).
- Cheng, N., Bao, P., Evans, S. D., Leggett, G. J. & Armes, S. P. Facile formation of highly mobile supported lipid bilayers on surface-quaternized pH-responsive polymer brushes. *Macromolecules* 48, 3095–3103 (2015).
- Chung, P. J., Hwang, H. L., Dasbiswas, K., Leong, A. & Lee, K. Y. C. Osmotic shock-triggered assembly of highly charged, nanoparticle-supported membranes. *Langmuir* 34, 13000–13005 (2018).
- Troutier, A.-L. & Ladavière, C. An overview of lipid membrane supported by colloidal particles. *Adv. Colloid Interf. Sci.* 133, 1–21 (2007).
- Ziaco, M. et al. Development of clickable monophosphoryl lipid a derivatives toward semisynthetic conjugates with tumor-associated carbohydrate antigens. J. Med. Chem. 60, 9757–9768 (2017).
- 100. Alam, S. et al. A clickable and photocleavable lipid analogue for cell membrane delivery and release. *Bioconjug. Chem.* 26, 1021–1031 (2015).
- 101. Li, M. et al. AFM studies of solid-supported lipid bilayers formed at a Au(111) electrode surface using vesicle fusion and a combination of Langmuir– Biodgett and Langmuir–Schaefer techniques. Langmuir 24, 10313–10323 (2008).
- 102. Su, Z., Goodall, B., Leitch, J. J. & Lipkowski, J. Ion transport mechanism in gramicidin A channels formed in floating bilayer lipid membranes supported on gold electrodes. *Electrochim. Acta* 375, 137892 (2021).
- 103. Mun, S. & Choi, S.-J. Optimization of the hybrid bilayer membrane method for immobilization of avidin on quartz crystal microbalance. *Biosens. Bioelectron*. 24, 2522–2527 (2009).

- 104. Smith, M. B., Tong, J., Genzer, J., Fischer, D. & Kilpatrick, P. K. Effects of synthetic amphiphilic α-helical peptides on the electrochemical and structural properties of supported hybrid bilayers on gold. *Langmuir* 22, 1919–1927 (2006).
- 105. Nikolov, V., Radisic, A., Hristova, K. & Searson, P. C. Bias-dependent admittance in hybrid bilayer membranes. *Langmuir* 22, 7156–7158 (2006).
- 106. Abbasi, F., Leitch, J. J., Su, Z., Szymanski, G. & Lipkowski, J. Direct visualization of alamethicin ion pores formed in a floating phospholipid membrane supported on a gold electrode surface. *Electrochim. Acta* 267, 195–205 (2018).
- 107. Wu, H.-L., Tong, Y., Peng, Q., Li, N. & Ye, S. Phase transition behaviors of the supported DPPC bilayer investigated by sum frequency generation (SFG) vibrational spectroscopy and atomic force microscopy (AFM). Phys. Chem. Chem. Phys. 18, 1411–1421 (2016).
- 108. Kett, P. J. N., Casford, M. T. L. & Davies, P. B. Sum frequency generation (SFG) vibrational spectroscopy of planar phosphatidylethanolamine hybrid bilayer membranes under water. *Langmuir* 26, 9710–9719 (2010).
- 109. Parikh, A. N., Beers, J. D., Shreve, A. P. & Swanson, B. I. Infrared spectroscopic characterization of lipid– alkylsiloxane hybrid bilayer membranes at oxide substrates. *Langmuir* 15, 5369–5381 (1999).
- Millo, D. et al. Characterization of hybrid bilayer membranes on silver electrodes as biocompatible SERS substrates to study membrane–protein interactions. *Colloids Surf. B* 81, 212–216 (2010).
  Plant, A. L., Brighamburke, M., Petrella, E. C. &
- 111. Plant, A. L., Brighamburke, M., Petrella, E. C. & Oshannessy, D. J. Phospholipid/alkanethiol bilayers for cell-surface receptor studies by surface plasmon resonance. Anal. Biochem. 226, 342–348 (1995).
- 112. Twardowski, M. & Nuzzo, R. G. Phase dependent electrochemical properties of polar self-assembled monolayers (SAMs) modified via the fusion of mixed phospholipid vesicles. *Langmuir* 20, 175–180 (2004).
- 113. Twardowski, M. & Nuzzo, R. G. Molecular recognition at model organic interfaces: electrochemical discrimination using self-assembled monolayers (SAMs) modified via the fusion of phospholipid vesicles. *Langmuir* 19, 9781–9791 (2003).
- 114. Nam, D.-H. et al. Molecular enhancement of heterogeneous CO<sub>2</sub> reduction. *Nat. Mater.* 19, 266–276 (2020).
- Chen, B. W. J. & Mavrikakis, M. Effects of composition and morphology on the hydrogen storage properties of transition metal hydrides: insights from PtPd nanoclusters. *Nano Energy* 63, 103858 (2019).
   Bhandari, S., Rangarajan, S. & Mavrikakis, M.
- Bhandari, S., Rangarajan, S. & Mavrikakis, M.
   Combining computational modeling with reaction kinetics experiments for elucidating the in situ nature of the active site in catalysis. *Acc. Chem. Res.* 53, 1893–1904 (2020).
   Liao, S., Holmes, K.-A., Tsaprailis, H. & Birss, V. I.
- 117. Liao, S., Holmes, K.-A., Tsaprailis, H. & Birss, V. I. High performance PtRulr catalysts supported on carbon nanotubes for the anodic oxidation of methanol. *J. Am. Chem. Soc.* 128, 3504—3505 (2006).
- 118. Liu, T. et al. Exceptional capacitive deionization rate and capacity by block copolymer based porous carbon fibers. Sci. Adv. 6, eaaz0906 (2020).
- 119. Liu, T., Zhou, Z., Guo, Y., Guo, D. & Liu, G. Block copolymer derived uniform mesopores enable ultrafast electron and ion transport at high mass loadings. Nat. Commun. 10, 675 (2019).
- 120. Ryu, J. et al. Thermochemical aerobic oxidation catalysis in water can be analysed as two coupled electrochemical half-reactions. *Nat. Catal.* 4, 742–752 (2021).
- 742–752 (2021).
  121. Haider, R. et al. High temperature proton exchange membrane fuel cells: progress in advanced materials and key technologies. *Chem. Soc. Rev.* 50, 1138–1187 (2021).
- Liang, J. et al. Ferrocene-based metal-organic framework nanosheets as a robust oxygen evolution catalyst. Angew. Chem. Int. Ed. 60, 12770–12774 (2021).
- 123. Liu, M. et al. Enhanced electrocatalytic CO<sub>2</sub> reduction via field-induced reagent concentration. *Nature* **537**, 382–386 (2016).
- 124. Dinh, C.-T. et al. CO<sub>2</sub> electroreduction to ethylene via hydroxide-mediated copper catalysis at an abrupt interface. *Science* 360, 783–787 (2018).
- 125. Xia, C. et al. General synthesis of single-atom catalysts with high metal loading using graphene quantum dots. *Nat. Chem.* 13, 887–894 (2021).
- 126. Cutsail, G. E., Ross, M. O., Rosenzweig, A. C. & DeBeer, S. Towards a unified understanding of the

- copper sites in particulate methane monooxygenase: an X-ray absorption spectroscopic investigation. *Chem. Sci.* **12**, 6194–6209 (2021).
- 127. Cutsail, G. E. III, Gagnon, N. L., Spaeth, A. D., Tolman, W. B. & DeBeer, S. Valence-to-core X-ray emission spectroscopy as a probe of O–O bond activation in Cu<sub>2</sub>O<sub>2</sub> complexes. *Angew. Chem. Int. Ed.* 58, 9114–9119 (2019).
- 128. Wuttig, A., Yoon, Y., Ryu, J. & Surendranath, Y. Bicarbonate is not a general acid in Au-catalyzed CO<sub>2</sub> electroreduction. J. Am. Chem. Soc. 139, 17109–17113 (2017).
- 129. Marshall-Roth, T. et al. A pyridinic Fe-N<sub>4</sub> macrocycle models the active sites in Fe/N-doped carbon electrocatalysts. *Nat. Commun.* 11, 5283 (2020).
- 130. Yan, B., Concannon, N. M., Milshtein, J. D., Brushett, F. R. & Surendranath, Y. A membrane-free neutral pH formate fuel cell enabled by a selective nickel sulfide oxygen reduction catalyst. *Angew. Chem. Int. Ed.* 56, 7496–7499 (2017).
- 131. Liu, M. et al. Atomically dispersed metal catalysts for the oxygen reduction reaction: synthesis, characterization, reaction mechanisms and electrochemical energy applications. *Energy Environ.* Sci. 12, 2890–2923 (2019).
- 132. Atwa, M. et al. Scalable nanoporous carbon films allow line-of-sight 3D atomic layer deposition of Pt: towards a new generation catalyst layer for PEM fuel cells. *Mater. Horiz.* 8, 2451–2462 (2021).
- 133. Tse, E. C. M., Schilter, D., Gray, D. L., Rauchfuss, T. B. & Gewirth, A. A. Multicopper models for the laccase active site: effect of nuclearity on electrocatalytic oxygen reduction. *Inorg. Chem.* 53, 8505–8516 (2014).
- 134. Mondol, P. & Barile, C. J. Four-electron electrocatalytic O<sub>2</sub> reduction by a ferrocene-modified glutathione complex of Cu. ACS Appl. Energy Mater. 4, 9611–9617 (2021)
- Varnell, J. A. et al. Identification of carbon-encapsulated iron nanoparticles as active species in non-precious metal oxygen reduction catalysts. *Nat. Commun.* 7, 12582 (2016).
- 136. Xia, C. et al. Continuous production of pure liquid fuel solutions via electrocatalytic CO<sub>2</sub> reduction using solid-electrolyte devices. *Nat. Energy* 4, 776–785 (2019).
- 137. Schreier, M., Yoon, Y., Jackson, M. N. & Surendranath, Y. Competition between H and CO for active sites governs copper-mediated electrosynthesis of hydrocarbon fuels. *Angew. Chem. Int. Ed.* 57, 10221–10225 (2018).
- 138. Verma, S., Lu, S. & Kenis, P. J. A. Co-electrolysis of CO₂ and glycerol as a pathway to carbon chemicals with improved technoeconomics due to low electricity consumption. *Nat. Energy* 4, 466–474 (2019).
- 139. Chen, X. et al. Electrochemical CO<sub>2</sub>-to-ethylene conversion on polyamine-incorporated Cu electrodes. *Nat. Catal.* 4, 20–27 (2021)
- Nat. Catal. 4, 20–27 (2021).

  140. Pan, H. & Barile, C. J. Electrochemical CO<sub>2</sub> reduction to methane with remarkably high Faradaic efficiency in the presence of a proton permeable membrane. Energy Environ. Sci. 13, 3567–3578 (2020).
- Pan, H. & Barile, C. J. Bifunctional nickel and copper electrocatalysts for CO<sub>2</sub> reduction and the oxygen evolution reaction. *J. Mater. Chem. A* 8, 1741–1748 (2020)
- 142. Darcy, J. W., Kolmar, S. S. & Mayer, J. M. Transition state asymmetry in C–H bond cleavage by protoncoupled electron transfer. J. Am. Chem. Soc. 141, 10777–10787 (2019).
- 143. Bullock, R. M. et al. Using nature's blueprint to expand catalysis with Earth-abundant metals. *Science* 369, eabc3183 (2020).
- 144. Ding, S. et al. Hemilabile bridging thiolates as proton shuttles in bioinspired H<sub>2</sub> production electrocatalysts. *J. Am. Chem. Soc.* 138, 12920–12927 (2016).
- 145. Hsieh, C.-H. et al. Redox active iron nitrosyl units in proton reduction electrocatalysis. *Nat. Commun.* 5, 3684 (2014).
- 146. Chan, S. I. & Yu, S. S. F. Copper protein constructs for methane oxidation. *Nat. Catal.* **2**, 286–287 (2019).
- 147. Wang, Y., Wang, D. & Li, Y. A fundamental comprehension and recent progress in advanced Pt-based ORR nanocatalysts. SmartMat 2, 56–75 (2021).
- 148. Wang, Q., Shang, L., Sun-Waterhouse, D., Zhang, T. & Waterhouse, G. Engineering local coordination environments and site densities for high-performance Fe-N-C oxygen reduction reaction electrocatalysis. SmartMat 2, 154–175 (2021).
  149. Costentin, C., Di Giovanni, C., Giraud, M., Savéant, J.-M.
- [49. Costentin, C., Di Giovanni, C., Giraud, M., Saveant, J.-M. & Tard, C. Nanodiffusion in electrocatalytic films. Nat. Mater. 16, 1016 (2017).

- 150. Thiyagarajan, N. et al. A carbon electrode functionalized by a tricopper cluster complex: overcoming overpotential and production of hydrogen peroxide in the oxygen reduction reaction. *Angew. Chem. Int. Ed.* 57, 3612–3616 (2018).
- Du, L. et al. Electrocatalytic valorisation of biomass derived chemicals. *Catal. Sci. Technol.* 8, 3216–3232 (2018).
- 152. Wei, Z. et al. Steering electron—hole migration pathways using oxygen vacancies in tungsten oxides to enhance their photocatalytic oxygen evolution performance. Angew. Chem. Int. Ed. 60, 8236–8242 (2021).
- 153. Tse, E. C. M. & Gewirth, A. A. Effect of temperature and pressure on the kinetics of the oxygen reduction reaction. *J. Phys. Chem. A* 119, 1246–1255 (2015). 154. Mo, X., Chan, K. C. & Tse, E. C. M. A scalable
- 154. Mo, X., Chan, K. C. & Tse, E. C. M. A scalable laser-assisted method to produce active and robust graphene-supported nanoparticle electrocatalysts. *Chem. Mater.* 31, 8230–8238 (2019).
- 155. Du, L. et al. Low-PGM and PGM-free catalysts for proton exchange membrane fuel cells: stability challenges and material solutions. *Adv. Mater.* 33, 1908232 (2021).
- 156. Chen, Z., Vannucci, A. K., Concepcion, J. J., Jurss, J. W. & Meyer, T. J. Proton-coupled electron transfer at modified electrodes by multiple pathways. *Proc. Natl Acad. Sci. USA* 108, E1461–E1469 (2011).
- 157. Weinberg, D. R. et al. Proton-coupled electron transfer. *Chem. Rev.* **112**, 4016–4093 (2012)
- 158. Li, P., Soudackov, A. V., Koronkiewicz, B., Mayer, J. M. & Hammes-Schiffer, S. Theoretical study of shallow distance dependence of proton-coupled electron transfer in oligoproline peptides. J. Am. Chem. Soc. 142, 13795–13804 (2020).
- Warburton, R. E. et al. Interfacial field-driven protoncoupled electron transfer at graphite-conjugated organic acids. J. Am. Chem. Soc. 142, 20855–20864 (2020)
- 160. Tse, E. C. M., Hoang, T. T. H., Varnell, J. A. & Gewirth, A. A. Observation of an inverse kinetic isotope effect in oxygen evolution electrochemistry. ACS Catal. 6, 5706–5714 (2016).
  161. Tse, E. C. M., Varnell, J. A., Hoang, T. T. H. &
- 161. Tse, E. C. M., Varnell, J. A., Hoang, T. T. H. & Gewirth, A. A. Elucidating proton involvement in the rate-determining step for Pt/Pd-based and nonprecious-metal oxygen reduction reaction catalysts using the kinetic isotope effect. *J. Phys. Chem. Lett.* 7, 3542–3547 (2016).
- 162. Roubelakis, M. M., Bediako, D. K., Dogutan, D. K. & Nocera, D. G. Proton-coupled electron transfer kinetics for the hydrogen evolution reaction of hangman porphyrins. *Energy Environ. Sci.* 5, 7737–7740 (2012).
- 163. Chang, C. J., Chang, M. C. Y., Damrauer, N. H. & Nocera, D. G. Proton-coupled electron transfer: a unifying mechanism for biological charge transport, amino acid radical initiation and propagation, and bond making/breaking reactions of water and oxygen. *Biochim. Biophys. Acta* 1655, 13–28 (2004).
- 164. Costentin, C. Proton-coupled electron transfer catalyst: heterogeneous catalysis. application to an oxygen evolution catalyst. ACS Catal. 10, 7958–7967 (2020).
- 165. Agarwal, R. G. et al. Free energies of proton-coupled electron transfer reagents and their applications. *Chem. Rev.* 122, 1–49 (2022).
- 166. Morris, W. D. & Mayer, J. M. Separating proton and electron transfer effects in three-component concerted proton-coupled electron transfer reactions. *J. Am. Chem. Soc.* 139, 10312–10319 (2017).
- 167. Gautam, R. P. & Barile, C. J. Preparation and electrontransfer properties of self-assembled monolayers of ferrocene on carbon electrodes. *J. Phys. Chem. C* 125, 8177–8184 (2021).
- 168. Chidsey, C. E. D. Free energy and temperature dependence of electron transfer at the metal-electrolyte interface. *Science* 251, 919–922 (1991).
  169. Pohl, E. E., Peterson, U., Sun, J. & Pohl, P. Changes
- 169. Pohl, E. E., Peterson, U., Sun, J. & Pohl, P. Changes of intrinsic membrane potentials induced by flip-flop of long-chain fatty acids. *Biochemistry* 39, 1834–1839 (2000).
- Kamp, F. & Hamilton, J. A. pH gradients across phospholipid membranes caused by fast flip-flop of un-ionized fatty acids. *Proc. Natl Acad. Sci. USA* 89, 11367–11370 (1992).
- 171. Grifall-Sabo, J. C., Nolan, T., Beck, M. M. & Barile, C. J. Kinetic modeling of electrocatalytic oxygen reduction products from lipid-modified electrodes. *J. Math. Chem.* 57, 2195–2207 (2019).
- 172. Mennel, J. A., Pan, H., Palladino, S. W. & Barile, C. J. Electrocatalytic CO<sub>2</sub> reduction by self-assembled

- monolayers of metal porphyrins. *J. Phys. Chem. C* **124**, 19716–19724 (2020).
- 173. Devadoss, A. & Burgess, J. D. Detection of cholesterol through electron transfer to cholesterol oxidase in electrode-supported lipid bilayer membranes. *Langmuir* 18, 9617–9621 (2002).
- 174. Ratajczak, M. K., Chris, Ko,Y. T., Lange, Y., Steck, T. L. & Lee, K. Y. C. Cholesterol displacement from membrane phospholipids by hexadecanol. *Biophys. J.* 93, 2038–2047 (2007).
- 175. Ege, C., Ratajczak, M. K., Majewski, J., Kjaer, K. & Lee, K. Y. C. Evidence for lipid/cholesterol ordering in model lipid membranes. *Biophys. J.* 91, L01–L03 (2006)
- Johnson, D. L. & Martin, L. L. Controlling protein orientation at interfaces using histidine tags: an alternative to Ni/NTA. J. Am. Chem. Soc. 127, 2018–2019 (2005).
- 177. Rusling, J. F. & Nassar, A. E. F. Enhanced electron transfer for myoglobin in surfactant films on electrodes. J. Am. Chem. Soc. 115, 11891–11897 (1993).
- Fleming, B. D. et al. Redox properties of cytochrome P450<sub>BM3</sub> measured by direct methods. *Eur. J. Biochem.* 270, 4082–4088 (2003).
- 179. Göpel, W. & Heiduschka, P. Interface analysis in biosensor design. *Biosens. Bioelectron.* 10, 853–883 (1995).
- Laftsoglou, T. & Jeuken, L. J. C. Supramolecular electrode assemblies for bioelectrochemistry. *Chem. Commun.* 53, 3801–3809 (2017).
- 181. Jeuken, L. J. C. Electrodes for integral membrane enzymes. *Nat. Prod. Rep.* **26**, 1234–1240 (2009)
- 182. Torchut, E., Bourdillon, C. & Laval, J.-M. Reconstitution of functional electron transfer between membrane biological elements in a two-dimensional lipidic structure at the electrode interface. *Biosens. Bioelectron.* 9, 719–723 (1994).
- 183. Marchal, D., Pantigny, J., Laval, J. M., Moiroux, J. & Bourdillon, C. Rate constants in two dimensions of electron transfer between pyruvate oxidase, a membrane enzyme, and ubiquinone (coenzyme Q8), its water-insoluble electron carrier. *Biochemistry* 40, 1248–1256 (2001).
- 184. Burgess, J. D., Rhoten, M. C. & Hawkridge, F. M. Cytochrome c oxidase immobilized in stable supported lipid bilayer membranes. *Langmuir* 14, 2467–2475 (1998).
- 185. Hemmatian, Z. et al. Electronic control of H<sup>+</sup> current in a bioprotonic device with gramicidin A and alamethicin. Nat. Commun. 7, 12981 (2016). This work illustrates the integration of complex transmembrane ion channels into HBMs for the construction of functional bioprotonic devices.
- 186. Kozuch, J., Steinem, C., Hildebrandt, P. & Millo, D. Combined electrochemistry and surface-enhanced infrared absorption spectroscopy of gramicidin A incorporated into tethered bilayer lipid membranes. Angew. Chem. Int. Ed. 51, 8114–8117 (2012). This work demonstrates the use of advanced surface spectroscopic techniques for the in situ structural and functional characterization of HBMs with membrane-bound peptides.

- 187. Langecker, M., Arnaut, V., List, J. & Simmel, F. C. DNA nanostructures interacting with lipid bilayer membranes. Acc. Chem. Res. 47, 1807–1815 (2014).
- 188. Radu, V., Frielingsdorf, S., Evans, S. D., Lenz, O. & Jeuken, L. J. C. Enhanced oxygen-tolerance of the full heterotrimeric membrane-bound [NiFe]-hydrogenase of *Ralstonia eutropha. J. Am. Chem. Soc.* 136, 8512–8515 (2014).
- Pollheimer, P. et al. Reversible biofunctionalization of surfaces with a switchable mutant of avidin. *Bioconjug. Chem.* 24, 1656–1668 (2013).
   Janiak, M. J., Small, D. M. & Shipley, G. G.
- 190. Janiak, M. J., Small, D. M. & Shipley, G. G. Temperature and compositional dependence of the structure of hydrated dimyristoyl lecithin. *J. Biol. Chem.* 254, 6068–6078 (1979).
- Gudmand, M. et al. Influence of lipid heterogeneity and phase behavior on phospholipase A<sub>2</sub> action at the single molecule level. *Biophys. J.* 98, 1873–1882 (2010).
- Moraille, P. & Badia, A. Enzymatic lithography of phospholipid bilayer films by stereoselective hydrolysis. J. Am. Chem. Soc. 127, 6546–6547 (2005).
- 193. Liu, J. & Conboy, J. C. Phase transition of a single lipid bilayer measured by sum-frequency vibrational spectroscopy. J. Am. Chem. Soc. 126, 8894–8895 (2004).
- 194. Yang, J. & Appleyard, J. The main phase transition of mica-supported phosphatidylcholine membranes. J. Phys. Chem. B 104, 8097–8100 (2000).
- 195. Feng, Z. V., Spurlin, T. A. & Gewirth, A. A. Direct visualization of asymmetric behavior in supported lipid bilayers at the gel-fluid phase transition. *Biophys. J.* 88, 2154–2164 (2005).
- 196. Hønger, T., Jørgensen, K., Biltonen, R. L. & Mouritsen, O. G. Systematic relationship between phospholipase A<sub>2</sub> activity and dynamic lipid bilayer microheterogeneity. *Biochemistry* 35, 9003–9006 (1996).
- 197. Ray, S., Scott, J. L. & Tatulian, S. A. Effects of lipid phase transition and membrane surface charge on the interfacial activation of phospholipase A<sub>2</sub>. *Biochemistry* 46, 13089–13100 (2007)
- 198. Wu, H. et al. Enzyme-catalyzed hydrolysis of the supported phospholipid bilayers studied by atomic force microscopy. *Biochim. Biophys. Acta* 1828, 642–651 (2013)
- 642–651 (2013). 199. Dufrēne, Y. F. & Lee, G. U. Advances in the characterization of supported lipid films with the atomic force microscope. *Biochim. Biophys. Acta* 1509, 14–41 (2000).
- 200. Leidy, C. et al. Membrane restructuring by phospholipase A<sub>2</sub> is regulated by the presence of lipid domains. *Biophys. J.* 101, 90–99 (2011).
   201. El Kirat, K., Morandat, S. & Dufrēne, Y. F. Nanoscale
- El Kirat, K., Morandat, S. & Dufrêne, Y. F. Nanoscale analysis of supported lipid bilayers using atomic force microscopy. *Biochim. Biophys. Acta* 1798, 750–765 (2010).
- Nagle, J. F. & Tristram-Nagle, S. Structure of lipid bilayers. *Biochim. Biophys. Acta* 1469, 159–195 (2000).
- 203. Leidy, C., Kaasgaard, T., Crowe, J. H., Mouritsen, O. G. & Jørgensen, K. Ripples and the formation of anisotropic lipid domains: imaging two-component

- supported double bilayers by atomic force microscopy. *Biophys. J.* **83**, 2625–2633 (2002).
- Leidy, C., Mouritsen, O. G., Jørgensen, K. & Peters, G. H. Evolution of a rippled membrane during phospholipase A, hydrolysis studied by time-resolved AFM. *Biophys. J.* 87, 408–418 (2004)
- 87, 408–418 (2004).
  205. Wang, W. & Tse, E. C. M. Proton removal kinetics that govern the hydrogen peroxide oxidation activity of heterogeneous bioinorganic platforms. *Inorg. Chem.* 60, 6900–6910 (2021).
- 206. Basu Ball, W., Neff, J. K. & Gohil, V. M. The role of nonbilayer phospholipids in mitochondrial structure and function. *FEBS Lett.* **592**, 1273–1290 (2018).
- Vanni, S., Hirose, H., Barelli, H., Antonny, B. & Gautier, R. A sub-nanometre view of how membrane curvature and composition modulate lipid packing and protein recruitment. Nat. Commun. 5, 4916 (2014).

#### Acknowledgements

E.C.M.T. thanks the Hong Kong (HK) Research Grants Council (RCC) for funding the HBM research programme via an Early Career Scheme (RCC grant 27301120) and the National Natural Science Foundation of China for providing a Young Scientists Fund (NSFC 22002132) to support research efforts on heterogeneous energy catalysis. The authors thank the CAS-RCC Joint Laboratory Funding Scheme (RCC grant JLFS/P-704/18) for supporting the HKU-CAS Joint Laboratory on New Materials. The authors acknowledge financial support from the Innovation and Technology Commission (ITC) for funding the "Laboratory for Synthetic Chemistry and Chemical Biology" via the Health@InnoHK programme. H.-L.W. thanks MOST (the Ministry of Science and Technology), Taiwan and the Center of Atomic Initiative for New Materials, National Taiwan University, from the Featured Areas Research Center Program within the framework of the Higher Education Sprout Project by the Ministry of Education in Taiwan (10819008). The contributions of C.J.B. and R.P.G. are based upon work supported by the National Science Foundation CAREER Award under grant number CHE-2046105.

#### **Author contributions**

All authors contributed equally to the preparation of this manuscript.

#### Competing interests

The authors declare no competing interests.

#### Peer review information

Nature Reviews Chemistry thanks Jwa-Min Nam and the other, anonymous, reviewer(s) for their contribution to the peer review of this work.

#### Publisher's note

Springer Nature remains neutral with regard to jurisdictional claims in published maps and institutional affiliations.

Springer Nature or its licensor holds exclusive rights to this article under a publishing agreement with the author(s) or other rightsholder(s); author self-archiving of the accepted manuscript version of this article is solely governed by the terms of such publishing agreement and applicable law.

© Springer Nature Limited 2022